Polymer Chemistry

Accepted Manuscript

ROYAL SOCIETY OF CHEMISTRY

www.rsc.org/polymers

Latex routes to graphene-based nanocomposites

Elodie Bourgeat-Lami,[a*] Jenny Faucheu,[b*] Amélie Noël [a, b]

[a] Université de Lyon, Univ. Lyon 1, CPE Lyon, CNRS, UMR 5265, Laboratoire de Chimie, Catalyse, Polymères et Procédés (C2P2), LCPP group, 43, Bd. du 11 Novembre 1918, F-69616 Villeurbanne, France

[b] Ecole Nationale Supérieure des Mines, SMS-EMSE, CNRS : UMR 5307, LGF, 158 cours Fauriel, 42023 Saint Etienne, France

Abstract

This review article describes recent advances in the elaboration of graphene-based colloidal nanocomposites through the use of graphene or graphene oxide in heterophase polymerization systems. Two main routes are reviewed: latex blending and *in situ* polymerization. In the first strategy, a segregated network is formed by confining the graphenic fillers in the interstices between the latex particles during the drying process. The morphology of the network depends on the relative dimensions of the fillers and the latex particles and on the interfacial interactions. The various approaches used to promote latex/graphene interactions via charge attractions or pi stacking are reviewed. The second method relies on the *in situ* formation of polymer latexes in the presence of graphenic fillers using emulsion, miniemulsion or suspension polymerization processes in the presence or absence of stabilizer. The use of graphene oxide as Pickering stabilizer and the effect of the dimensional characteristics of the graphene sheets on particles morphology are also discussed. At last, a brief discussion of mechanical and electrical properties of graphene-latex nanocomposites with regards to the characteristics of the filler and the latex-graphene relative dimensions is given to provide insight into the main requirements of graphenic fillers with respects to various applications.

Key words: graphene, (reduced) graphene oxide, heterophase polymerization, electrical, mechanical properties

1. Introduction

1.1. Brief Historical Background

Graphene is a pure carbon compound that is virtually transparent and completely flexible. At only one-atom thick, it is also the thinnest material ever created. Graphene is considered as the fundamental building block for graphitic materials of all other dimensions. It can be wrapped up into zero-dimensional (0D) fullerenes, rolled into one-dimensional (1D) nanotubes and stacked into three-dimensional (3D) graphite. Long-range π-conjugation in graphene yields extraordinary thermal, mechanical, and electrical properties, which have long been the interest of many theoretical studies and more recently became an exciting area for experimentalists. Although graphene has been the subject of theoretical studies for more than 60 years, historically, graphene became well-known when Nobel prize was awarded to Prof. Andre K. Geim and Prof. Konstantin S. Novoselov, at the University of Manchester, UK, and the Institute for Microelectronics Technology, Chernogolovka, Russia for their experimental studies on graphene sheets that were isolated from graphite using adhesive tape.[1] Since this breakthrough, increasingly more researchers have started experimental studies on graphene characterizations and applications. In particular, one promising application of graphene is in polymer nanocomposites, in which nanoscale fillers are incorporated into a polymer matrix. Pristine graphene as well as graphene derivatives such as graphene oxide and functionalized graphene oxide have been explored, all aiming at enhancing the final properties of the composite material in terms of conductivity, mechanical properties and other functional properties such as gas barrier properties.

1.2. Scope and Previous Reviews

Graphene is un-doubtfully one of the most remarkable substances ever discovered. Graphene can be prepared with unique purity and exhibits some remarkable properties: in particular a highly efficient electrical conductivity combined with an extremely fast charge transport and an extraordinary strength. These properties make graphene-based products potentially useful in a wide range of applications like in electronics (high speed transistors, one electron transistors) and in materials science (composite materials). Given its many attractive features, it is not surprising that graphene has become a very hot topic for scientists these last ten years. Since the Nobel Prize awarded to A. K. Geim, K. S. Novoselov in 2010, the number of articles and patents on graphene and graphene-related materials has shown uninterrupted

growth. According to a recent report from Thomson Reuters, there are no signs that research on graphene is slowing. Similarly, and for the same reasons, the number of review articles dealing with graphene has also increased. These reviews cover a wide range of topics including synthesis (using physical, chemical or electrochemical approaches),[2] exfoliation methods,[3] surface modification,[4] physical properties,[5] and the elaboration of composite materials.[6] Moreover, it may be noted that these topics are strongly interconnected, and are consequently often covered all together in a single article.[7]

Early studies on graphene-based composite materials mainly focused on the preparation of intercalated or exfoliated nanocomposites. The properties of graphene-based nanocomposites have often been reported to be superior to those of clay or carbon nanotubes (CNTs) polymer composites. Indeed, although CNTs show comparable mechanical properties to graphene, the later exhibits superior thermal and electrical conductivity properties. Such outstanding properties are most often ascribed to a strong graphene platelets / matrix interface and the establishment of a 3D graphene network. Various processing routes such as melt intercalation, solution blending or *in situ* intercalative polymerization have been explored to get optimized dispersion of graphitic fillers into polymer matrices and improve filler/matrix interactions. Among them, the use of polymer latex particles has received increasing attention. Polymer latexes are produced by polymerization in dispersed media (*e.g.*, emulsion, miniemulsion, suspension[8] and dispersion polymerizations) where the most important technique is emulsion polymerization. Emulsion polymerization offers significant advantages as compared to bulk or solution polymerization owing to the better control of heat and viscosity of the medium along with the possibility of increasing the molecular weight of the polymer chains without affecting the rate of polymerization. In the last twenty years, polymerization in dispersed media have proven highly suitable for the production of polymer/inorganic particles to generate a variety of composite colloids.[9] These can be further processed into films with improved mechanical, thermal or barrier properties compared with their pure-polymer counterparts. Although graphene is technically not an inorganic compound, their incorporation into latex suspensions involves similar concepts. The topic of graphene-based colloidal materials has been briefly addressed by Thickett *et al.*[10] in an extensive review covering the functionalization of graphene oxide (GO) by controlled radical polymerization and its subsequent incorporation into polymeric materials. The elaboration of GO-based composite particles through colloidal templating or the use of GO as a colloidal surfactant in emulsion or miniemulsion polymerization processes were also reviewed in this article but only marginal attention was paid to the latex blending strategy and to the final materials

properties. *In situ* emulsion polymerization techniques and latex blending were also briefly mentioned in some other review papers[6a, 6d, 6e, 6g, 11] but again in a non-exhaustive way.

The present review intends to give the current state-of-the-art developments in the synthesis of graphene-based nanocomposites using latex technology (section 4 and 5) with a focus on the preparative methods and processing. Then an emphasis on the structure-property relationships will be presented in section 6. As a starting point, graphene specifications and general considerations on polymerization in dispersed media will be briefly described in the following sections.

2. General considerations on graphene fillers

The formal definition of graphene is a two-dimensional monolayer of carbon atoms closely packed in a honeycomb lattice (Figure 1a). Graphite comprises a large number of graphene monolayers stacked into a three-dimensional structure and Few Layer Graphene (FLG) is defined as stacks of 2 to 20 graphene layers (Figure 1b). Graphene has a theoretical Van der Waals (VdW) thickness of 0.34 nm, and is the thinnest two-dimensional nanofiller reported so far.[2a]

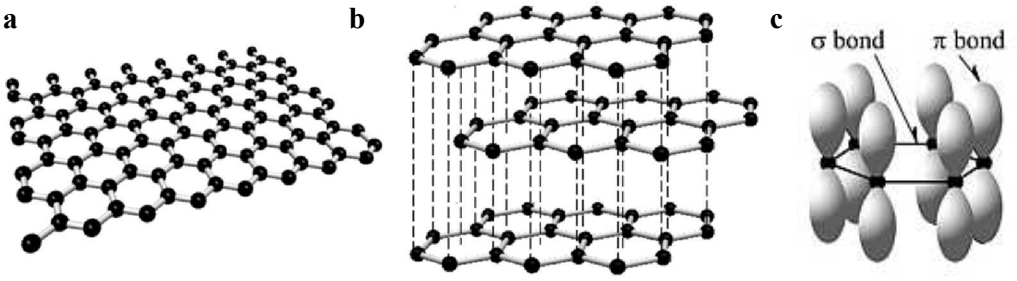

Figure 1. a) Graphene structure, b) stacking of graphene layers and c) distribution of σ and π bonds on the graphene structure. Reproduced from ref. [12] with permission from Intech.

Within graphene, one σ-orbital and two in-plane π-orbitals of carbon are associated with sp^2 hybridization.[13] The π bonds, available both above and below each graphene layer (Figure 1c), can overlap with those from neighboring carbon atoms. The σ-electrons are tightly bound and cannot significantly contribute to electrical conductivity, but the π and π* orbitals can behave like valence bands and conduction bands and induce planar conduction mechanism.[14]

Graphene also exhibits an extremely high aspect ratio usually 10^4 or higher, and high intrinsic flexibility.

To be used in composite elaboration, graphene has to be produced in rather large amounts. Thus, techniques such as adhesive tape peeling, epitaxial growth and chemical vapor deposition are inadequate. For composite elaboration, graphene fillers are produced through two main processes using graphite as raw material. First, a multistep chemical process that takes advantage of the fact that oxidized graphite is more easily exfoliated that pristine graphite. After oxidation, the graphite oxide suspension is easily exfoliated using mechanical or ultrasound methods into graphene oxide (GO). However, as GO is non conductive, a reduction step is required to recover electrically conductive properties. Second, liquid phase exfoliation is a mechanical process that consists in peeling graphite flakes in suspension using ball milling. While enabling to produce larger amounts of graphene, these elaboration processes make trade-offs in graphene surface quality (presence of surface defects) and graphene stacking (FLG).

2.1. Production of graphene fillers through Hummer's method

The most popular method used to produce graphene is a three-step process: i) oxidation of graphite, ii) exfoliation of graphite oxide into GO, and iii) reduction of GO. This method is often called "Hummer's method" after his work[15] on graphite chemical oxidation. In 1958, Hummer performed the oxidation of graphite with potassium permanganate and nitric acid in concentrated sulfuric acid. Since, various solvents[16] have been used such as water,[17] acetone,[18] *N*-methylpyrrolidone (NMP)[19,20] or tetrahydrofuran (THF).[21] The oxidation time and the amount of oxidants influence the size of GO sheets.[22] After the oxidation step, exfoliation into GO is performed through ultrasonication. The surface of the GO exhibits oxygen-containing moieties such as carboxylic, hydroxyl and epoxy groups (Figure 2).

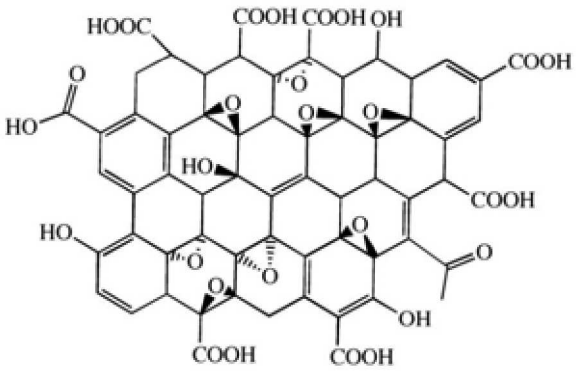

Figure 2. Scheme of oxygen-containing moieties on the surface of GO. Reproduced from ref. [23] with permission from Scientific & Academic Publishing.

As GO is dielectric, a reduction step is performed after exfoliation to recover electrical conductivity properties. The reduced compound is called reduced graphene oxide (RGO). Various techniques have been developed to perform the reduction step. The chemical reduction using hydrazine is the most common route, but hydrazine toxicity has prompted researchers to develop new reducing agents, such as sulfur compounds,[24] hydroxylamine[25] or vitamin C[26] to obtain graphene suspensions in water. When using organic solvents, solvothermal reduction in NMP[27] or via gamma-ray radiation[28] have been proposed. To counteract the restacking of RGO during reduction[7], surfactants or polymeric stabilizers may therefore be added for further stabilization. For example, Stankovich et *al.*[29] used sodium poly(styrene sulfonate) (PSSNa) to stabilize GO platelets during reduction with hydrazine. The reduction of GO can also be achieved thermally, at high temperatures (1050 °C), or electrochemically.[5b] The reduction process influences the final electrical properties of the graphene sheets[30]. Cheng *et al.*[31] reviewed the impact of various non chemical GO reduction processes on sheet resistance (Figure 3) and showed that the sheet conductance of pristine graphene cannot be fully recovered after reduction. Defects on the RGO surface such as non-conjugated sp^3 carbon atoms represent most of the defects at the surface of RGO and remaining oxygen-containing groups affect the final electrical properties. Note that these remaining defects could facilitate further RGO functionalization and dispersion with polymers. [32]

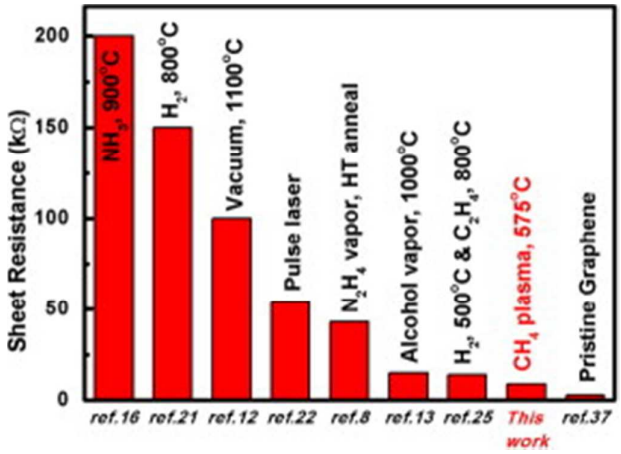

Figure 3. Impact of the GO reduction process on the sheet resistance. Reproduced from ref. [31] with permission from Elsevier.

Hummer's method typically enables the production of RGO with a lateral size between 200 nm and a few μm and comprising 1 to 10 graphene layers. As an alternative to Hummer's method, liquid phase exfoliation, presented below, enables the production of few-layer graphene (FLG), which consists of 2 to 20 layers of graphene stacked together and exhibiting micron scale lateral size.

2.2. Production of graphene fillers through liquid phase exfoliation of graphite

Liquid phase exfoliation aims at producing FLG through direct exfoliation of graphite flakes. Contrary to Hummer's method, neither oxidation nor reduction steps are needed. However as strong VdW interactions bind graphene layers together, the exfoliation of graphite in solution requires high-energy input. Sonication and ball milling in water or organic solvent have been studied for this purpose. Sonication has been demonstrated as a decent exfoliation procedure in a liquid with a surface tension similar to that of graphite. Scission induced by sonication can break large crystallites into smaller crystallites and vibration can chip off thin 2D nanosheets from the outer surfaces of layered materials.[20] To minimize the energy cost associated with exfoliation, graphite can be sonicated in organic solvents with surface energy close to that of graphene such as NMP.[33] The addition of an intercalation compound, like in potassium-intercalated graphite, KC_8,[34] can also help the exfoliation of graphite and favor high concentrations of graphene in suspensions.[35] The introduction of positive or negative charges between the graphite layers can promote exfoliation and stabilization of the sheets in organic or aqueous media. For instance, small molecules, such 1-pyrenecarboxylic acid, can

interact with graphene via π-π stacking.[36] The use of surfactant can be efficient[37] to produce FLG suspensions with micron-size graphene (lateral) and typical graphene concentrations around 1 mg mL^{-1}. For instance, Guardia *et al*.[38] used an non-ionic surfactant (Tween-80), Lotya *et al*.[39] chose sodium dodecyl benzene sulfate (SDBS) and Lee et *al.*[40] combined SDBS with fluorinated intercalation compounds.

In ball-milling, graphite flakes is added to a liquid medium and injected in the rotating reactor containing milling beads (usually zirconia) in close-pack circuit. The high shear energy of the ceramic beads produces the exfoliation and break of the graphite flakes. Similarly to sonication, considerations on surface energy can be taken into account to stabilize the graphite and the resulting graphene flakes. Low yield was observed in dimethyl formamide (DMF)[36] while Knieke *et al*.[41] proposed to produce FLG in water using SDS as surfactant leading to FLG suspensions (around 1 mg mL^{-1}) with micron-size lateral dimensions and low number of stacked layers.

Compared to Hummer's method, the liquid phase exfoliation process requires less toxic chemical products but a large amount of graphite flakes. Hummer's method is multistep while liquid phase exfoliation is rather straightforward and regarding dimensional specifications of FLG, thicknesses are of similar order of magnitude while lateral size is smaller for the mechanical method. It is worth noticing that both Hummer's method and liquid phase exfoliation can be performed in water phase, meaning that these processes are well compatible with further composite latex elaboration.

2.3. Properties of graphenic fillers

Ideal graphene exhibits exceptional mechanical,[42] optical,[43] electronic,[44] and thermal properties.[45] However in composite elaboration, non-ideal graphene is used. The word "graphene" is often used as a generic term to qualify graphenic compounds such as FLG or RGO.[46] Table 1 highlights the differences in terms of properties between a graphene monolayer, which can be almost considered as a "model material" and FLG that is closer to a "real material" that can be produced under industrial conditions. Values for the intrinsic conductivity of graphene monolayers are largely documented in the literature and have been reported to be around 10^7-10^8 S m^{-1} for in-plane conductivity. It was demonstrated that in-plane conductivity decreases with increasing the number of graphene layers due to overlapping of the non-hybridized p_z orbitals perpendicular to the sheets. The addition of one layer to a monolayer was found to divide by half the conductivity while further addition had a

lower influence.[47] Thus the intrinsic conductivity of FLG is expected to be around 10^6-10^7 S m^{-1}. An increase of the number of graphene layers will also induce a decrease of the elastic modulus, thermal conductivity and a small increase of the opacity.

Table 1. Physical properties of a graphene monolayer and FLG.

Properties	Monolayer graphene	Few-Layer Graphene (FLG)
Elastic modulus	1 TPa [48]	0.5 TPa [49]
Thermal conductivity	5.1 10^3 W mK^{-1} [45]	5-25 10^1 W mK^{-1} [50]
Electrical conductivity	10^7 S m^{-1} [51]	10^6-10^7 S m^{-1} [47]
Optical properties	2.3 % of opacity [52]	16 % of opacity[53]

2.4. Surface Functionalization of Graphenic Fillers

Current methods for graphene production lead to graphene layers with so-called defects. Defects are structural imperfections and chemical impurities randomly distributed on the face or edges of the graphene sheet.[54] These defects reduce the intrinsic electrical properties but can also provide additional reactive sites for further graphene functionalization. In addition, the graphene edges are considered to be more reactive than the inner surface faces.[4d] Finally, a graphene sheet exhibits reactive sites on its edges and defects (Figure 4). It is also expected that zigzag edges will display higher reactivity compared to armchair ones. However, it is technically challenging to control the edge structure, so, in practice, graphene contains a combination of both types of edge configurations (combined edge), which makes it difficult to control the functionalization process.[55] Numerical simulations[56] indicate that hydroxyl, carboxyl, or other groups can easily be attached to vacancy-type defects. The same holds true for graphene edges that are normally saturated with hydrogen.[57]

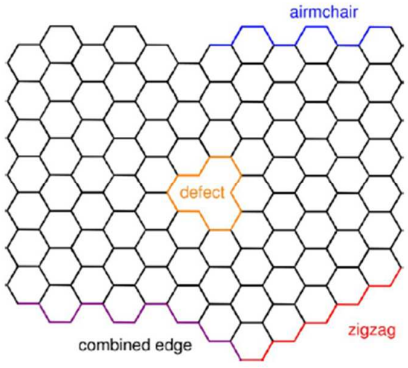

Figure 4. Scheme representing the reactive sites on graphene sheets. Reproduced from ref. [4d] with permission from the American Chemical Society.

In brief, the functionalization of graphene sheets might result from unpaired electrons enhancing the reactivity there and leading to a chain reaction from the initial point of attack.[58] Due to the presence of unpaired electrons available on the graphene, the carbon compounds are currently used as trapping agent.[59,60] In fact, radical polymerizations of vinyl monomers are remarkably retarded in the presence of nano-carbons, such as carbon black, carbon nanotubes, and fullerene, because initiator radicals and growing polymer radicals are readily trapped by these nano-carbons.[61,62]

GO had also been used for trapping of polymer radicals for functionalization with styrene, for example, as described by Beckert *et al*.[63] The presence of radicals can also interact with the polymer initiators during *in situ* polymerization in the presence of nano-carbon compounds. It was reported that during the polymerization initiated by conventional radical initiators in the presence of carbon black, a part of the polymer formed is grafted onto the carbon surface. The percentage of grafted polymer is however less than 10%. Most of trapped radicals are initiator fragments instead of polymer chains.[61] The retardation or inhibition of the polymerization, due to the presence of nano-carbon compounds, strongly depends on the nature of the monomers.[64] An inhibition was first observed in the polymerization of styrene with carbon black. In fact, the growing polymer chains are more reactive toward the carbon black surface than the initiator fragments and the growth of polymer is stopped prematurely during this induction period. Whereas, in the case of methyl methacrylate or vinyl acetate polymerization, a marked retardation of the polymerization was visible due to the predominant reaction of the initiator fragments with the carbon black surface. The possible interactions of the graphene surfaces with the initiators and monomers can create a modification of the polymerization rate. Furthermore, the presence of radicals on the graphene surface can lead to the creation of covalent bonds between the graphene platelets and the growing polymer without upstream functionalization of graphene platelets.

Graphene and FLG can be functionalized through covalent and non-covalent (VdW, electrostatic, π-π stacking) approaches.[65,66] Non-covalent approaches involves, for instance, the use of end-functionalized polymer chains with pyrene groups to favor π-π stacking interactions with graphene platelets.[6e, 67] In the covalent method, the carboxylic and hydroxyl groups can be used for functionalization[6e,68,69] through, for instance, amination,[70] esterification,[71] isocyanate-grafting[72] or polymer grafting.[73]

3. General Features of Polymerization in Heterogeneous Dispersed Media

Heterophase polymerization systems can be defined as two-phase systems in which the resulting polymer and/or starting monomer are in the form of a fine dispersion in an immiscible liquid medium called the "polymerization medium", "continuous phase" or "outer phase". Even if oil-in-water (o/w) systems are greatly preferred on an industrial scale, water-in-oil (w/o) systems can also be employed for specific purposes. Heterogeneous polymerization processes can be classified as emulsion, miniemulsion, suspension, dispersion or precipitation systems according to the initial state of the polymerization mixture, the kinetics of polymerization, the mechanism of particle formation and the size and shape of the final polymer particles. As heterophase polymerization processes are central to this review article, they will be briefly described below.

3.1. Suspension Polymerization

Suspension polymerization is essentially a bulk polymerization in which the reaction mixture is suspended as droplets in an aqueous continuous phase.[74] Therefore, the initiator, monomer and polymer must be insoluble in water. The suspension mixture is prepared by addition of a monomer solution containing dissolved initiator into the pre-heated aqueous suspension medium. Droplets of the organic phase are formed and maintained in suspension by the use of (i) vigorous agitation throughout the reaction and (ii) hydrophilic macromolecular stabilizers dissolved in water (*i.e.*, low molar mass polymers such as poly(vinyl alcohol), poly(*N*-vinylpyrrolidone) or hydroxymethylcellulose). Each droplet acts as a small bulk polymerization reactor in which the normal kinetics apply. Polymer is produced in the form of beads whose average diameters are close to those of the initial monomer droplets (0.01 to 2 mm) even if inadvertent droplet breaking and coalescence widen the bead size distribution. Polymer beads are easily isolated by filtration provided they are rigid and not tacky. Therefore, the suspension polymerization process is unsuitable for preparing polymers that have low glass transition temperatures (T_g). It is widely used for styrene (St), methyl methacrylate (MMA), vinyl chloride and vinyl acetate (VAc) monomers which corresponding polymers display high T_gs.

3.2. Emulsion Polymerization

Emulsion polymerization is an important industrial process for the production of latex paints, rubbers, coatings and adhesives.[75] In "conventional" emulsion polymerization, polymer particles are formed by starting with an insoluble (or scarcely soluble) monomer emulsified with the aid of a surfactant present at a concentration above its CMC. The monomer is originally distributed between coarse emulsion droplets, surfactant micelles and the water phase (where a small proportion of monomer is molecularly dissolved). The initiator is soluble in water (although partially water-soluble initiators which partition between the oil and aqueous phases, like for instance 2,2'-azobis(isobutyronitrile) (AIBN), can also be used), which leads to a very different particle formation mechanism compared with suspension systems.

Polymerization starts in the aqueous phase by the formation of free radicals through the initiator thermolysis and the addition of the first monomer units. These oligomeric radical species are rapidly captured by the monomer-swollen micelles, where propagation is supported by absorption of monomer diffusing from the monomer droplets through the aqueous phase to maintain equilibrium. Therefore, stabilized nuclei are produced to give primary particles, which grow gradually until the monomer is completely consumed. The number of primary latex particles formed, and the time during which they grow, determine the final particle size. Polymer particles synthesized by emulsion polymerization generally have final diameters in the range of 50–600 nm, *i.e.*, considerably smaller than those made by suspension polymerization.

In emulsifier-free polymerizations, the polymerization is carried out in the same manner as described above, except that no surfactant is used. Nucleation occurs by oligoradical precipitation into unstable nuclei, which collide to form larger particles. Polymerization takes place mainly within these monomer-swollen particles and particles grow similarly to conventional emulsion polymerization. Quite recently, it has been shown that inorganic solids can be exploited to replace surfactants, leading to the formation of inorganic-armored latexes. This solids-stabilized emulsion polymerization process has been successfully implemented using a large variety of inorganic particles such as silica,[76,77] clays,[78,79] and iron oxide.[80]

Polymers prepared by emulsion polymerization are used either directly in the latex form or after isolation by coagulation or spray drying of the latex. They are used as binders in paints, adhesives, paper coatings, carpet backings, water-based inks, non-woven textiles, and related applications. They are also used as supports for medical diagnostics. Critical parameters in all these applications are the particle size, the presence of appropriate end groups on the particle

surface (for covalent bonding of targeted molecules in biomedical applications or for adhesion to a given substrate in coatings), and the stability of the colloidal suspension.

3.3. Miniemulsion Polymerization

Miniemulsion polymerization is conceptually similar to a suspension polymerization, but employs much smaller monomer droplets which lead to polymer particles in the submicron size range.[81] Ideally, every monomer droplet is directly converted into a polymer particle, with negligible exchange of species between particles. Due to the small droplets size, the initiator can be either oil- or water-soluble.

In a first step, miniemulsion droplets of 50–300 nm are formed by applying high shear (via a high pressure homogenizer or ultrasound) to a system containing the dispersed phase, the continuous phase, a surfactant, and a hydrophobe. The hydrophobe acts as an osmotic pressure agent for preventing the interdroplet mass transfer phenomenon known as Ostwald ripening. Polymer particles are obtained by direct conversion of monomer droplets, with their final size tunable by controlling the shearing conditions and therefore the initial droplet size. One of the main advantages of miniemulsion polymerization is its versatility; it is for example applicable to non-radical polymerizations, and the encapsulation of resins, liquids and a multitude of preformed particles. Armored structures have also been recently attained via the polymerization of Pickering stabilized miniemulsion droplets[82,83] (which will be hereafter referred to as "Pickering miniemulsion polymerization") following the discovery of Ramsden and Pickering that finely-divided insoluble solid particles can efficiently stabilize emulsions.[84]

3.4. Precipitation and Dispersion Polymerization

In precipitation polymerization, the reaction mixture is initially homogeneous like in solution polymerization, but it acts as a precipitant for the growing polymer. The initially formed macromolecules therefore collapse and coagulate to create particle nuclei, which gradually flocculate into irregularly shaped and polydisperse particles. This process is for example used for the synthesis of polytetrafluoroethylene (PTFE) in water and polyacrylonitrile (PAN) in bulk.

In dispersion polymerization, the polymerization medium is not a precipitant but a poor solvent for the resulting polymer.[85] Thus, the macromolecules swell rather than precipitate, and the polymerization proceeds largely within these individual particles to generate more monodisperse products than in precipitation systems. To ensure particle stability,

macromolecular stabilizers have to be used (as in suspension polymerization). The diameters of the polymer particles are in the 0.5–10 μm range, which is generally much larger than in emulsion polymerization, although small polymer particles (100–500 nm) can also be obtained by employing reactive stabilizers or block copolymers.

4. Graphene-based Nanocomposites via Physical Blending

Composite materials produced by blending latexes with fillers are environmentally preferable to solvent-based alternatives as no volatile organic substances are released during film formation. In addition, compared to melt processing or solution blending, enhanced properties at lower filler content can be reached as a result of the excluded volume created by the polymer particles that forces the fillers into interstitial spaces between the polymer particles during drying. This process leads to a specific arrangement of the fillers into the polymer matrix defined as the "segregated network" and has been explored to fabricate graphene-based composites. The morphology of the segregated network naturally depends on the relative dimensions of the latex and the filler. If the lateral size of the graphenic filler (w_{RGO}) is smaller than the latex diameter (d_{latex}), a segregated network with a morphology driven by the latex particles is obtained,[86,87,88,89,90] *i.e.* a cellular morphology with graphene walls and polymer cells as illustrated in Figure 5.

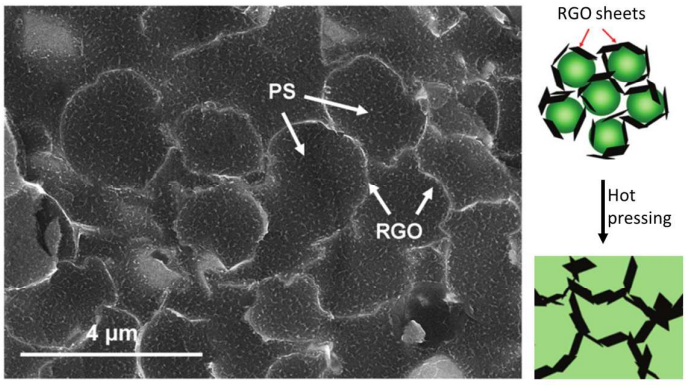

Figure 5. Scanning electron microscopy (SEM) image of the cross-section of a polystyrene (PS)/RGO composite blend (d_{latex} = 3 μm and w_{RGO} = 1 μm). Adapted from ref. [87] with permission of the Royal Society of Chemistry.

It is worth noticing that contrary to clay fillers - also widely explored to produce latex-based composites - graphenic fillers are compliant sheets that commonly adopt wavy or wrinkled structures[91] once dispersed in a polymer matrix. Thus, when graphene fillers are few times larger than the latex particles, the graphene sheet tends to wrap the polymer particle so that a cellular morphology[86-87,88,92,93,94,95] is also expected as illustrated in Figure 6.

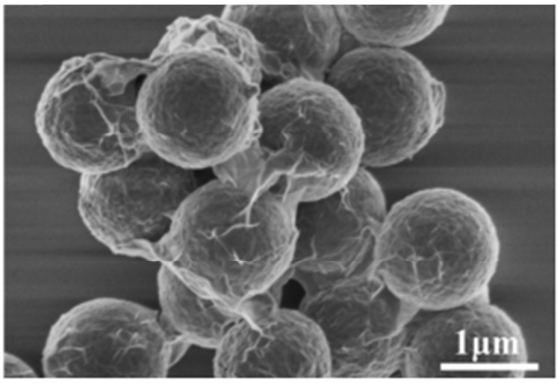

Figure 6. SEM image of PS/RGO composite (d_{latex} = 3 µm and w_{RGO} = 200 nm to few µm) showing that graphene sheets are compliant and tend to wrap the polymer particles. Reproduced from ref. [95] with permission from Elsevier.

Finally, if the lateral size of the graphenic filler is strongly larger than the latex diameter, a segregated network also forms even though the large graphene sheets tend to link or wrap several latex particles together[96,97,98,99] as illustrated in Figure 7. With fillers carrying such high aspect ratio, self-alignment might occur at high filler content, due to steric hindrance of the wide graphene sheets as observed by Yousefi *et al.*[100]

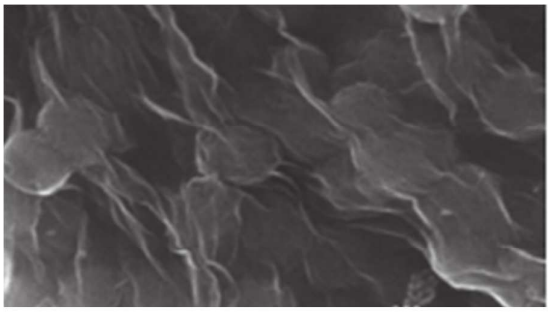

Figure 7. SEM image of PS/RGO composite (d_{latex} = 150-200 nm and w_{RGO} = several µm) showing graphene sheets wrapping and bridging several latex particles. Reproduced from ref. [96] with permission from Elsevier.

Many kinds of conductive composite particles have been fabricated through self-assembly mechanism, promising to provide a facile and versatile way to the assembly of small particles, and to control the functionality in such colloidal systems. Two main strategies have been reported in literature: i) GO is blended with the latex followed by reduction to recover the electrical properties, or ii) RGO or pristine FLG is blended with the latex, *i.e*. the reduction step (if needed) occurs prior to the blending step. Both strategies have drawbacks and advantages. On the one hand, GO is hydrophilic and is highly negatively charged due to the presence of oxygen functional groups such as phenolic hydroxyls and carboxylic acids on the surface and edges. GO sheets can be dispersed in water and can be easily mixed with a latex leading to a stable suspension but the reduction step is critical as RGO is hydrophobic and hardly stable in water. The reduction step tends to destabilize the suspension, so the filler distribution and the composite morphology have to be secured during this step. On the other hand, using directly RGO or pristine FLG prevents the need of a reduction step, but again to secure the composite morphology, the blending step needs specific conditions. Thus, the main challenges in producing efficient graphene-based composites through latex blending lie on two key factors: first secure the cellular morphology and second perform high reduction level of GO (if GO is used as intermediate compound).

In their review article on graphene-polymer nanocomposites for structural and functional applications, Hu *et al*.[6d] focused on the choice of the polymer matrix. Benefiting from almost infinite choices of monomers, oligomers, and chemistries available, polymer matrices can be precisely tuned and controlled to exhibit the whole spectrum of physiochemical properties. Among the large variety of polymeric matrices for advanced nanocomposites; elastomers, thermoplastics, epoxies, block copolymers, and hydro/aerogels are used widely due to their unique physical and chemical properties, which can be tailored to various applications and specific needs. For example, elastomers are highly stretchable polymers consisting of lightly cross-linked long chains. In contrast, epoxy resins contain rigid segments and are very heavily cross-linked so that their mechanical strength, stiffness, as well as their brittleness, are extremely high. Thermoplastic polymers exhibit lower mechanical properties but can be reinforced by crystalline domains, and are not chemically cross-linked so they can be processed, shaped, melted, and recycled. Therefore, the choice of polymer matrix also impacts the final properties of graphene-based composites. The following section is arranged into sub-sections differentiating the thermoplastic from the cross-linked matrices. The discussion focuses on the ability to enhance the filler distribution in the polymer matrix and secure the cellular morphology but also on the reduction level of GO if used as intermediate compound.

In addition, conductivity is a valuable qualitative measure of the two factors combined, i.e. the conversion of GO to RGO and filler spatial distribution. The enhancement of conductive properties and functional properties will be further discussed in Section 6.

4.1. Thermoplastic Polymeric Latexes blended with GO Suspensions

As GO is hydrophilic and easily dispersible in water, nanocomposites fabrication through latex blending could be a rather straightforward process. However, the reduction step could be critical in terms of suspension stability, morphology control but also reduction efficiency. Wang *et al.*[101] noticed through Raman spectra analysis that the presence of the polypropylene (PP) latex gave rise to a slight decrease in the reduction efficiency of GO in their RGO/PP composites prepared by mixing the PP latex with an exfoliated GO aqueous dispersion and subsequently reduced the GO nanosheets in the presence of hydrazine followed by filtration. During the reduction step, hydrophilic GO became hydrophobic RGO as a result of the disappearance of oxygen-containing groups from the surface. Despite this drastic interfacial change, the final microstructure could be secured by tuning an adequate interaction between the filler and the latex particles to form a precipitate or coagulant exhibiting a composite microstructure. In most of the works reviewed hereafter, the final composite material was obtained through drying or filtration followed by hot compression molding of the solid parts.

For instance, Long *et al.*[87] used poly(*N*-vinylpyrrolidone) (PVP)-grafted PS microspheres to secure GO on the surface via hydrogen bonding. SEM observations supported the hypothesis that the affinity between the GO sheets on PVP- grafted PS microspheres was strong enough to immobilize the GO sheets during the mild chemical reduction by a vitamin C solution. The final composite was obtained after hot pressing and its conductive properties were studied (Figure 8). XPS and conductivity measurements demonstrated that thermal reduction occurred during the hot pressing step; however the effectiveness was lower than chemical reduction. This process simplification paid the price of yielding a composite conductivity (0.5 S m^{-1} for 2 vol%) that was not as high as that for PS/RGO composites prepared with the vitamin C reduction (4.6 S m^{-1} for 2 vol%).

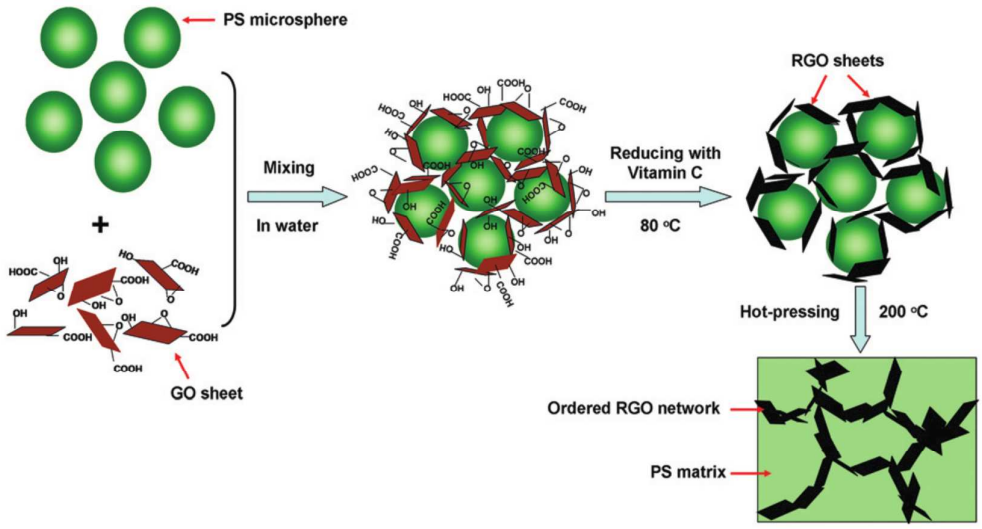

Figure 8. Scheme illustrating the preparation of PS/RGO composites with an ordered three-dimensional microcellular network by mixing GO sheets and PS microspheres, followed by GO reduction with vitamin C and hot pressing. Reproduced from ref. [87] with permission from the Royal Society of Chemistry.

Li *et al.*[97] fabricated graphene-based PS nanocomposites by mixing PS latex stabilized by SDBS with an aqueous dispersion of GO without any additional stabilizer. The mixture was intentionally coagulated with sodium chloride in order to produce composite micro-particles containing both the polymer beads and the GO sheets. Then, these micro-particles underwent *in situ* reduction into RGO using hydrazine hydrate (Figure 9). The final composite was obtained after drying the micro-particles, followed by hot pressing. XPS elemental analyses showed that performing the reduction step after the co-coagulation step was more efficient than the contrary. This was attributed to the fact that for the RGO-PS composite in which GO was reduced before co-coagulation, the graphene nanosheets tend to form a restacked structure as PS nanospheres are not adsorbed onto their surfaces. The glass transition temperature of the nanocomposites slightly shifted to a higher temperature with increasing graphene loading suggesting that the thermal stability of the nanocomposites was improved. In addition, the introduction of graphene resulted in a sharp decrease in the area under the damping peak, indicating that the segmental mobility of the PS chains during the glass transition was significantly limited and obstructed by the presence of graphene.

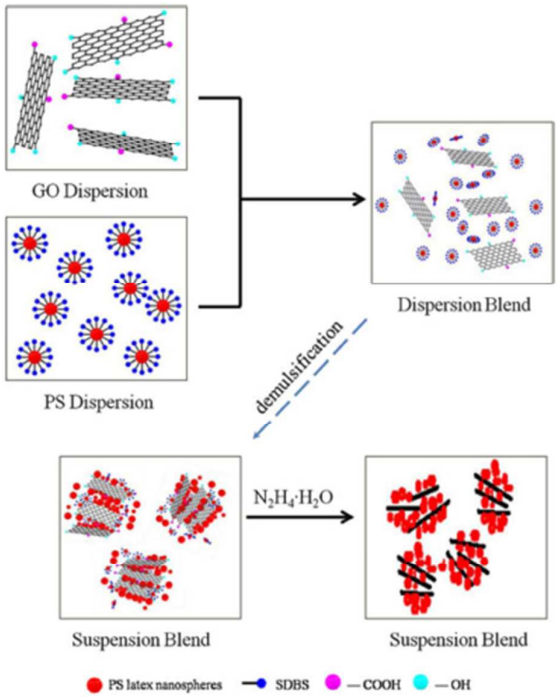

Figure 9. Scheme illustrating the preparation of PS/RGO composite microparticles by mixing GO and PS dispersions, followed by GO reduction with hydrazine hydrate. Reproduced from ref. [97] with permission from Springer.

Yousefi *et al.*[100] produced RGO/polyurethane (PU) composites. A GO dispersion was mixed with an aqueous PU emulsion to obtain a homogeneous colloidal dispersion of GO and PU, which was then chemically reduced. The resulting dispersion was stable for several months without any graphene aggregation, whereas the reduction of bare GO dispersion in the absence of PU resulted in significant agglomeration. It was hypothesized that the PU particles were adsorbed onto the RGO surface leading to a uniform, protective PU layer on the surface of the RGO sheets.

To secure the final segregated network morphology, self-assembly strategies have been reported with increasing complexity to favor interactions between the latex surface and the GO surface. The self-assembly process was driven by mutual electrostatic interactions between GO and polymer nanospheres but also chemical compatibilisation or surface functionalization have been explored.

As described earlier, GO in water is negatively charged; methods have been developed to render the surface of the latex positively charged to favor electrostatic self-assembly. For instance, some authors add cationic surfactants to cover the latex surface. Surfactants can be either non-ionic or ionic and adsorb onto the interfaces to stabilize hydrophobic particles

suspended in water, but the use of cationic surfactants induces the presence of positive charges on the surface of the latex. Zhang *et al*.[102] produced core–shell structured particles using GO as a shell material with poly(methyl methacrylate) (PMMA) latex with the use of a cationic surfactant: cetyl trimethylammonium bromide (CTAB). The GO-PMMA particles showed better thermal stability than that of the pure PMMA particles.

With a similar goal, another approach consists in using a cationic initiator. Pham *et al*.[99] prepared PMMA latex by surfactant-free emulsion polymerization using a cationic free radical initiator which creates the positive charges on the surface of the PMMA particles. In contrast, the GO sheet is highly negatively charged. The zeta potential (ZP) of the PMMA latex and the GO dispersion was found to be 34.9 mV and −43.4 mV, respectively. After hydrazine reduction, the PMMA-RGO precipitate was filtered. The size ratio allowed the RGO sheet to interpose itself between several PMMA particles. SEM images showed that crumpled and wrinkled RGO sheets were uniformly distributed in the PMMA matrix. The improvement in thermal stability of PMMA-RGO composites can be attributed to the formation of a high aspect ratio, inflammable RGO network in the polymer matrix, which acts as a barrier inhibiting the emission of the decomposition products during combustion. Significant enhancement in the storage modulus in both glassy and rubbery regions was observed. Moreover, a surfactant-free process was used resulting in high electrical properties.

Another strategy relies on grafting functional groups on the latex surface to render the surface positively charged. Wu *et al*.[96] grafted amine groups on the surface of PS nanospheres leading to surface charges switching from positive (zeta potential = + 26 mV) to negative (zeta potential = –29 mV) with increasing pH value from 2 to 11. When added to the GO suspension, spontaneous coagulation occurred at pH=4 while at pH=10, no aggregation occurred indicating that the electrostatic interaction was the driving force. In addition, at pH<1, no large aggregates were observed possibly due to protonation of GO. This result suggests that the mutual assembly should be triggered under weakly acidic medium. The resulting coagulum was filtered and reduced using hydrogen iodide (HI) solution, and finally made into films through hot compression molding. SEM images showed graphene sheets covering polymer spheres and linking neighboring spheres to form a 3D graphene framework in the coagulations. The hot-press process was found to be critical to generate compact junction contacts between RGO sheets in the 3D architecture.

Zhao *et al*.[95] synthesized positively charged polystyrene latex (PS+) through dispersion polymerization in an ethanol/water medium by using methacryloxyethyltrimethyl ammonium chloride as co-monomer. Due to the electrostatic adsorption and π–π interaction, GO

nanosheets gradually wrapped the surface of the cationic PS particles. For a pH range from 2 to 11, GO nanosheets presented negative charges (ZP = -44 mV to -53 mV) which may derive from the ionization of the corresponding carboxylic acid,[103] while the surface charge of the PS particles switched from positive (ZP = +41 mV) to negative (ZP = -54 mV) with a maximum ZP = +60.5 mV at pH 5. As the self-assembly could only be triggered when PS and GO were oppositely charged and considering that a higher ZP value results in a more stable aqueous dispersion, the chosen experimental conditions were: pH 5, ZP_{PS} = +60.5 mV and ZP_{GO} = -55.2 mV. SEM observations of a fracture surface showed a honeycomb-like 3D microstructure consisting of adjacent individual RGO sheets. The electrical conductivity of the composites increased significantly from 8.39 10^{-14} to 15.7 S/m when the RGO content increased from 0.02 to 0.81 vol%.

Gudarzi *et al.*[104] used acrylic acid as a hydrophilic monomer to form a polar shell at the surface of PMMA latex particles prior to the addition of GO suspension. Due to the strong bond between polar segments of polymer chains and oxygen groups of graphene, strong interfacial interaction was guaranteed, which rendered the colloidal polymer as both a stabilizer and compatibilizer. The resulting composite colloids remained stable during GO reduction, due to the molecular level dispersion of graphene in the resulting polymeric composite. XRD analyses confirmed that the presence of polymer particles prevent RGO from restacking after drying. Enhancement in modulus and hardness was measured and a notable shift of T_g toward higher temperatures was observed with addition of RGO. This latter was attributed to interaction at the molecular level and quite possibly formation of the hydrogen bonding among oxygen containing groups in the structure of graphene and polymer particles' surface.

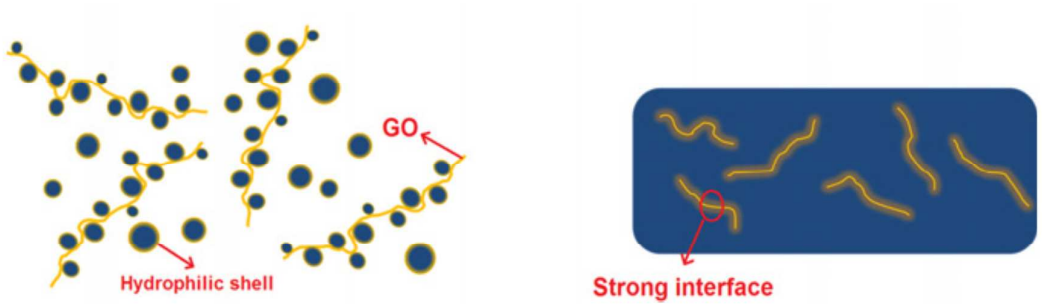

Figure 10. Scheme illustrating the formation of polymer/GO composites via latex blending and subsequent casting resulting in the creation of a high GO/polymer interfacial area. Reproduced from ref. [104] with permission from Elsevier.

Jiang *et al.*[98] prepared positively charged PTFE latex by grafting a polycationic polymer, polyethyleneimine (PEI). This procedure led to an increase in ZP from -20.7 mV (PTFE latex) to +25.6 mV (PEI grafted PTFE latex). PTFE/graphene composites were produced by an electrostatic self-assembly process where well-dispersed GO sheets having a negative charge were mixed with the positively charged PTFE latex followed by chemical reduction and hot sintering. The composites displayed higher mechanical properties but reduced ductility than pure PTFE. At 2 wt%, the electrical conductivity of the composite exceeded 1.5 S m^{-1}. A higher wear resistance but a lower friction coefficient was observed for the composite compared to pure PTFE.

Fan *et al.*[86] explored the electrostatic self-assembly process one step further by producing positively charged GO by formation of an amide bond between PEI and GO in addition to the common negatively charged GO suspension. With these two GO suspensions, PS microspheres were wrapped by GO sheets via layer-by-layer (LbL) assembly of oppositely charged GO sheets. The deposited GO was then reduced, and composite films with a graphene conductive network were prepared by hot pressing. Improvement in thermal stability has been observed.

Some authors also considered the addition of a third component with conductive properties. For instance, Tang *et al.*[90] proposed the use of CNTs as an aid to induce self-assembly of GO on PS microspheres. In this approach, GO was found to be an effective surfactant that could stabilize CNTs in water to yield a homogenous black dispersion. On the one hand, GO was used as an alternative stabilizer to otherwise insulating surfactants and wrapped PS microspheres acting as "nano-walls" to prevent CNTs from diffusing into the PS microsphere, in particular during hot pressing. GO was then reduced to conductive graphene to electrically connect with CNTs. On the other hand, CNTs on RGO served as effective spacers to prevent graphene from re-stacking even though at high filler concentration, re-stacking of RGO was observed. XPS results showed that most of the oxygen-containing groups were removed by the HI reduction process. The conductivity of the composite containing both CNTs and RGO was higher than that of the composites containing CNTs or RGO as the sole fillers, and enhancement of tensile modulus and strength was observed.

Zhang *et al.*[105] reported the synthesis of a conductive assembly consisting of PS microspheres, RGO, and Ag using silver nitrate ($AgNO_3$) as precursor. GO-coated PS microspheres were first prepared by hydrophobic and π–π interactions between GO and the PS microspheres. Due to the presence of hydroxyl groups, the surface of GO-coated PS microspheres possessed

a certain amount of negative charges that was favorable for Ag^+ adsorption. GO and Ag^+ were then simultaneously reduced. TEM and SEM observations showed a thin layer of RGO on the surface of PS microspheres, and some Ag nanoparticles stuck on the RGO, though partial convolution of RGO sheets on the PS microspheres led to some aggregated Ag nanoparticles. Higher thermal stability was observed.

Finally in another approach, Yang *et al.*[106] grafted atom transfer radical polymerization (ATRP) initiator molecules onto the GO sheets by reaction of 2-bromo-2-methylpropionyl bromide with the hydroxyl and amine groups. Poly(dimethylaminoethyl methacrylate) (PDMAEMA) chains were subsequently grown from the functionalized GO sheets by *in situ* ATRP at 60 °C using *N,N,N',N'',N''*-pentamethyldiethylenetriamine (PMDETA) as a ligand and CuBr. The resulting PDMAEMA-functionalized GO sheets could be readily exfoliated in water at pH 1, and were further decorated with poly(ethylene glycol dimethacrylate-*co*-methacrylic acid) (P(EGDMA-*co*-MAA)) particles which adsorbed on their surface via H-bonding interactions, therefore highlighting the ability to control morphology. However as no reduction was performed, one can question the influence of grafted polymer chains on the conductive properties of such RGO.

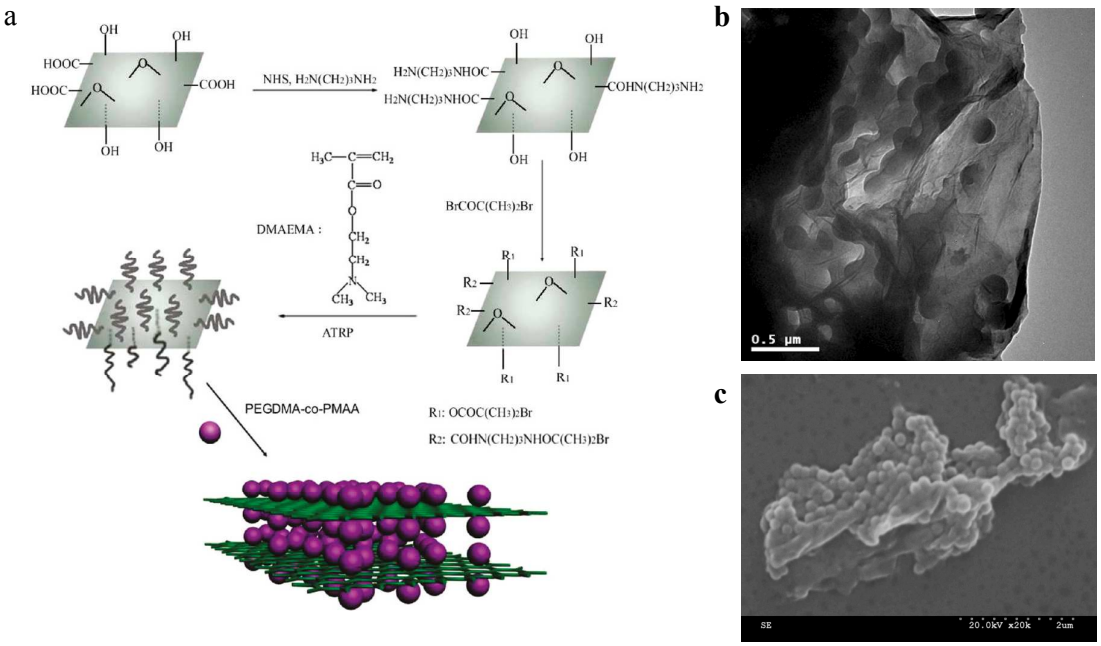

Figure 11. a) Scheme illustrating the grafting of PDMAEMA on GO sheets and their decoration by polymer particles. b) Transmission electron microscopy (TEM) and c) SEM images of exfoliated GO decorated by P(EGDMA-*co*-MAA) latex particles. Reproduced from ref. [106] with permission from the American Chemical Society.

4.2. Thermoplastic Polymeric Latexes blended with RGO or Graphene Suspensions

As discussed in Section 2, the reduction process does not fully reduce GO to graphene; this intermediate material is commonly referred to as RGO. As a consequence, the conductive properties of graphene are not fully recovered in RGO. Moreover, Wang *et al.*[101] showed that in GO/latex composites, the presence of the latex particles can give rise to a slight decrease in the reduction efficiency of GO. Thus, in order to favor high conductivity in the final composite, synthetic routes directly using graphene or RGO reduced prior to the latex blend step, have been explored. In this case, the challenge is that (contrary to GO) graphene and RGO are not stable in water without the aid of stabilizers. However, the presence of foreign stabilizers may also affect the conductivity of the nanocomposites by reducing charge transport within the conductive network. The planar aromatic structure of graphene can interact with surfactants with a hydrophobic tail containing planar or nearly planar polycyclic structures, unsaturated bonds and/or aromatic rings where strong π-π interactions are possible. A quite straightforward approach is to use SDBS surfactant as it is commonly used to stabilize carbon-based fillers, in particular graphene and RGO. Mechrez *et al.*[107] produced polyacrylate/graphene nanocomposites by dispersing graphene nanosheets in an aqueous dispersion of a commercial polyacrylate latex with SDBS surfactant followed by a microfiltration process. Ghislandi *et al.*[108] mixed a PP latex with a graphene dispersion stabilized by SDBS to a final filler content between 0.1 wt % and 10 wt %. Each mixture was freeze-dried and then hot pressed into films. In these two studies, water was rapidly extracted from the system in order to preserve the high dispersion level of the nanofillers within the polymer matrix successfully leading to conductive properties. However a cellular morphology was not reported. Besides, Noël *et al.*[88] produced poly(methyl methacrylate-*co*-*n*-butyl acrylate) (P(MMA-*co*-BA))/graphene nanocomposites using a surfactant-free latex mixed with a graphene suspension stabilized by SDBS. No coagulation was observed and free standing films could be obtained by natural water evaporation at 40°C. TEM observations showed that a cellular morphology was obtained and highly conductive properties were reached.

To better secure the cellular morphology, other stabilizers such as polymeric stabilizers have been explored. Polymeric stabilizers can be either non-ionic or ionic, and create physical or chemical interactions with carbon-based fillers, thus contributing to their stabilization through electrostatic or steric mechanisms. For instance, PVP is a stabilizer containing hydrophilic

pyrrolidone moieties, and a polyvinyl hydrophobic backbone. It can thus adsorb on hydrophobic surfaces and promote steric stabilization in aqueous solutions. Arzac *et al.*[93] produced a conductive composite by emulsion mixing. The composite morphology exhibited armored polymer particles with RGO platelets weakly bonded to the polymer, probably by hydrogen bonds formed between the polar polymeric particles and the hydrophilic (pyrrolidone) part of PVP adsorbed at the RGO surface. An electrical conductivity of 0.236 S m^{-1} was achieved for 0.9 vol% RGO.

Yoonessi *et al.*[89] prepared graphene/polycarbonate (PC) nanocomposites by latex blending and solution blending. The latex blending was performed by mixing a PC latex (from Sabic) with PVP and a graphene suspension stabilized with a non-ionic surfactant. Conductive graphene nanoparticles were positioned on the polycarbonate microsphere (Figure 12). An electrical conductivity of 10^{-2} S m^{-1} was achieved for 0.55 vol% RGO and enhancement of tensile modulus was observed.

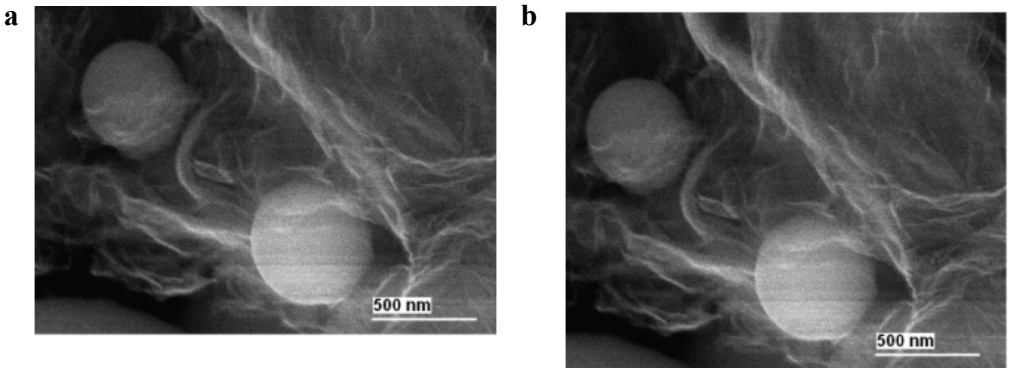

Figure 12. SEM images of graphene/PC composite materials containing a) 0.55 vol% and b) 1.1 vol% of graphene. Reproduced from ref. [89] with permission from the American Chemical Society.

In work by Pinto *et al.*[109], graphene nanoplatelets (GNP, commercial grade) were directly dispersed in a poly(vinyl acetate) (PVAc, commercial grade) latex without using additional surfactants or dispersants. The stability and non-agglomeration (Figure 13) of the composite dispersions were attributed to interaction of the graphene nanoplatelets with the protective colloids originally present in the commercial latex (typically poly(vinyl alcohol) (PVA) and hydroxyethylcellulose (HEC)). Improvement in adhesive bond strength was observed.

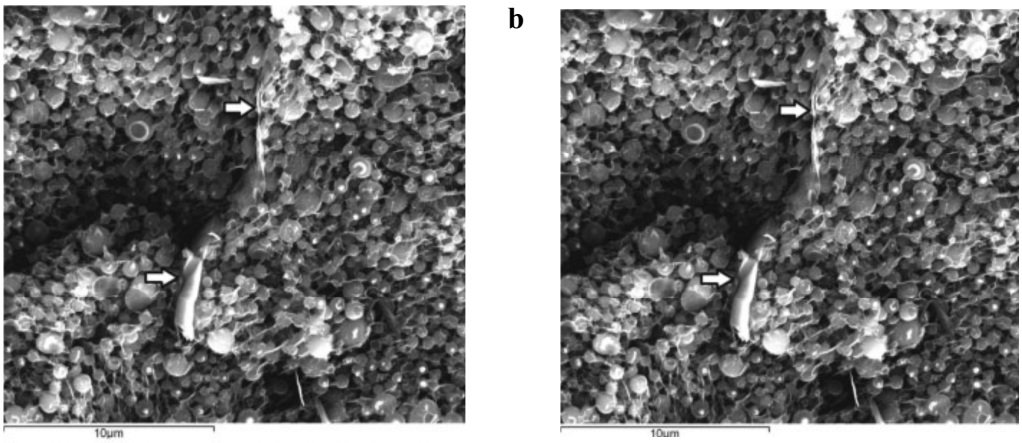

Figure 13. Cryo-SEM images of GNP/PVAc composite suspensions obtained by blending a PVAc latex with a) 0.3 wt% and b) 2 wt% of GNP. Reproduced from ref. [109] with permission from the Society of Chemical Industry.

Ju *et al.*[110] prepared partially charged RGO sheets by controlled chemical reduction of graphite oxide. After reduction, RGO showed the partial survival of polar groups including carboxylate anions and hydroxyl groups and the surface of the graphene sheets was consequently negatively charged (ZP = -36.01 mV). Then, positively charged PS beads of different sizes were prepared by emulsifier-free emulsion copolymerization with calcium stearate. After mixing, self-assembled hybrid spheres agglomerated and were deposited by spray-coating. SEM images showed that the polymer spheres were successfully decorated by graphene nanosheet. When reducing the diameter of cationic polymer spheres from 5 µm to 600 nm, graphene sheet could adhere on several polymer spheres rather than wrapping each sphere, resulting in ligament formation between neighboring spheres. The decrease of PS beads diameter induced an increase of conductivity, suggesting that the number of ohmic contact would be a critical factor determining electrical conductivity.

Polyelectrolytes can also be used as stabilizers. These are polymers containing multiple ionizable groups, which stabilize particles by electrostatic interactions. For instance, poly(styrene sulfonate) (PSS) is a polyelectrolyte composed of repeat units similar to the chemical structure of SDBS, and can effectively stabilize graphene platelets in water. Syurik *et al.*[111] reduced GO-sheets with hydrazine in the presence of PSS to produce graphene covered with PSS (PSS-graphene) after filtration and drying. For the preparation of the composites, the PSS-graphene was dispersed in water and mixed with PS or PP latexes prior to freeze-drying and compression molding. The lower melt viscosity and the crystallization of

the PP caused predominantly non-isotropic orientation of the GR nanofillers while isotropic orientation was observed in the RGO-PS composite. This morphology was confirmed by conductivity measurements in direction parallel and perpendicular to the sample top surface. To improve interaction between the filler and the polymer matrix, some authors have explored reactive interactions such as copolymerization or cross-linking. Spasevska *et al*.[112] produced waterborne P(MMA-*co*-BA)/RGO composites in which the polymer nanoparticles were functionalized with OH groups by introducing the functional comonomer 2-hydroxyethyl methacrylate (HEMA) in the monomer mixture. The blending technique was based on an emulsion mixing process, during which a water dispersible polyurethane cross-linker (containing free isocyanate functionalities on both chain ends) was added (Figure 14). The cross-linker bonded covalently to the polymer and the RGO to form a single complex hybrid structure. The bonding was established through spontaneous NCO reaction with OH functionalities present on both the surface of RGO platelets and the surface of the polymer nanoparticles. Higher amount of cross-linker promoted partial encapsulation of polymer particles by the RGO sheets, by bending the RGO sheets around the particles, creating more organized structure. The composites containing 1 wt% of RGO and medium amount of cross-linker showed the maximum electrical conductivity achieved in this study (0.1361 S m^{-1}) and a highly homogeneous distribution of RGO thus a kind of optimum combination of RGO and cross-linker amounts. When a higher amount of cross-linker was added, it was hypothesized that part of it remained free and was incorporated into the composite matrix, decreasing the conductivity and influencing the morphology. By decreasing the cross-linker content, the RGO platelets were randomly oriented in the matrix, less bended and more aggregated. It was hypothesized that the amount of cross-linker used was not enough to bind with the individual RGO sheets, which promoted aggregation between the non-bonded sheets. Consequently, the electrical conductivity of these composites dropped significantly. The composites, despite covalent bonding of the RGO sheets in the composite matrix, showed electrical conductivity properties and increase of Young's modulus was observed.

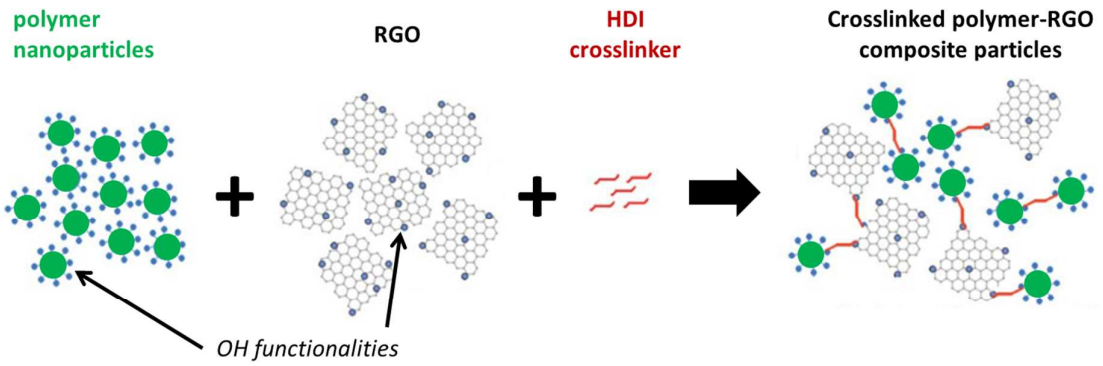

Figure 14. Scheme illustrating the reactive emulsion mixing procedure reported by Spasevska *et al*. using a water dispersible cross-linker to covalently bind OH-functionalized polymer nanoparticles and RGO platelets. Adapted from ref. [112] with permission from the Royal Society of Chemistry.

Jiang *et al.*[113] reported a one-step covalent functionalization and simultaneous reduction of GO with hydroxyethyl acrylate (HEA), resulting in graphene functionalized with double bonds. The functionalized graphene was used to covalently attach PMMA particles to the edges of graphene sheets (Figure 15a). This polymerization step is rather close to the *in situ* polymerization approaches described later in Section 5. Here, the PMMA particles acted as chemical compatibilizers (Figure 15b) effectively preventing filler agglomeration and markedly improving their dispersion in the PMMA matrix during the subsequent melt processing. The strong chemical interaction between the functionalized graphene sheets and the PMMA matrix, combined with the good dispersion in PMMA matrix enhanced the barrier effect of graphene. Improvement in thermal stability was observed. A shift in the glass transition temperature of PMMA towards higher temperatures was observed after incorporation of functionalized graphene, and was attributed to the restriction of polymer's chain motions, which indicates a strong interfacial interaction between the functionalized graphene sheets and the PMMA chains due to the formation of covalent bonds. Improvements of mechanical properties were reported.

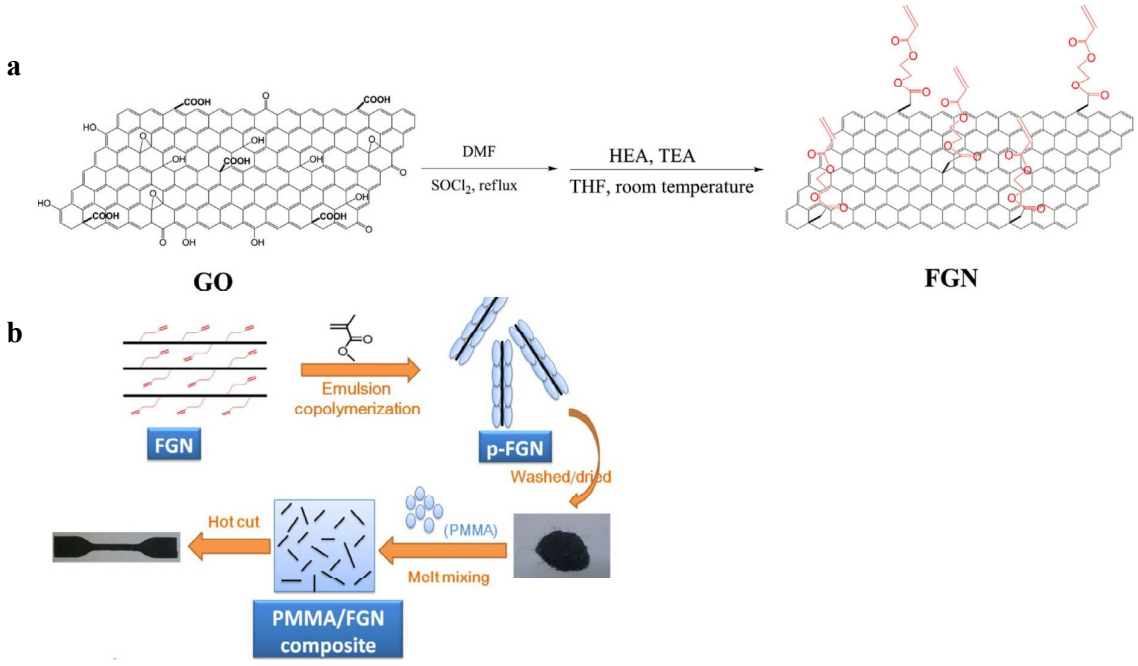

Figure 15. a) Scheme illustrating the synthesis of functionalized graphene (FGN) and b) schematic representation of the procedure used to prepare PMMA/FGN composite by *in situ* emulsion polymerization followed by melt blending. Reproduced from ref. [113] with permission from Elsevier.

In a last example, Tchernook *et al.*[114] studied a semi-crystalline system wherein aqueous high molecular weight linear polyethylene "nanocrystal"/graphene composite dispersions were produced *in situ* by ethylene insertion polymerization in water or alternatively via a post-polymerization technique. The precipitates were dried and melt processed prior to characterization. RGO was used without any prior compatibilizing surface modification. The small size of the polyethylene nanocrystals enabled a homogeneous distribution of graphene throughout the polymer matrix. High conductivities and low percolation thresholds were measured and were attributed to the morphology of the composites.

4.3. Cross-linked Polymer Matrices

Self-assembly approaches have been explored by several authors for cross-linked polymeric systems, in particular for natural rubbers (NR). NR latexes consist of particles of cis-1,4-polyisoprene core and phospholipids–protein shell without any specific electrostatic charges on the surface.[115] Similarly to thermoplastic-based systems, either GO or RGO can be used

during the blending step. However, in many applications, conductivity is not of primary focus and property enhancement also deals with water permeability and mechanical properties; thus no reduction is needed and the use of GO is quite straightforward. For instance, Matos et al.[92] simply mixed a GO dispersion with a NR latex prior to curing at 70 °C. For comparison purposes, the same authors also fabricated RGO-NR systems. To do so, GO was reduced and dispersed in water with CTAB prior to NR latex blending step. As unfilled NR, the biodegradability of graphene-based composites was verified. Regarding the swelling behavior, all the nanocomposite samples absorbed less solvent than the pure rubber and the more concentrated the nanocomposites were, the less solvent was absorbed. The degradation temperature of the GO-NR nanocomposites was quite similar to the one of the unfilled polymer, indicating that the presence of GO did not affect the thermal stability of the rubber. But in nanocomposites with RGO, a lower degradation temperature compared to pure NR was observed. This was associated with the presence of CTAB, which decomposes in the range 260–310 °C. To prevent the drawback of the presence of surfactant, Li *et al.*[116] proposed to prepare graphene-NRL composites by using ammonia as stabilizer. Ammonia diffused completely during the final heat vulcanization. First ammonia was added to pre-vulcanized NR latex and RGO suspensions prior to mixing. During this ionization stage, both NR particles and graphene sheets were negatively charged (the negative charges being balanced by ammonium counter-ions). The electrostatic repulsion between NR particles and graphene sheets enabled the homogenous dispersion of graphene sheets in the NR matrix. During the drying process, with the evaporation of water and ammonia, the viscosity increased fixing likewise the RGO sheets in the system while heat curing cross-linked the different NR particles together. An increase of 9% in tensile strength of the RGO-NR composite without compromising the elongation at break was observed. In addition, the glass transition temperature shifted toward a higher temperature, which was attributed to physical cross-linking of graphene.

Zhan *et al.*[117] and Yan *et al.*[118] prepared NR-based nanocomposites by direct blend of GO suspension with NR latex followed by chemical reduction and vulcanization. The mixture underwent coagulation and was dried prior to final processing. The final composite was either processed by static hot pressing or twin-roll mixing, followed by hot pressing. This latter process is commonly used in natural rubber industry, however it tends to destroy the segregated network morphology. Static hot pressing is therefore preferred to preserve the peculiar morphology (Figure 16). XPS, SAXS and NMR analyses showed that the RGO platelets affect the vulcanization process of natural rubber. In particular, polysulphidic sulphur

species were more prevalent in the samples with segregated morphology and increasing the RGO content reduced the presence of these species. The composites with a conductive segregated network displayed excellent water vapor barrier properties and good mechanical properties, enhancement of tensile strength but decrease of the strain at break. In another work, Zhan *et al.*[119] mixed a GO suspension and NR latex prior to chemical reduction and co-coagulation using formic acid to form composite particles. After filtration, the final composite was prepared in an open twin roll mill with addition of pure NR and curing agents. This process produced much better dispersion and exfoliation of RGO in the NR matrix and contributed to an increase in the tensile strength compared to the direct twin roll mixing of RGO and NR. Among three different carbonaceous fillers (carbon black, multi wall carbon nanotube, and RGO), GE was found to be the best one for reinforcing the NR. With the introduction of GE, the crosslink density increased and swelling ratio decreased. Potts *et al.*[120] also studied the two-roll mixing process. In this study, a latex premixing step was performed prior to the two-roll mixing step. Large property improvements were observed in these latex premixed nanocomposites compared to composites simply processed by the two-roll mixing process. This was attributed to a more uniform dispersion of the RGO platelets, coupled with a larger accessible interfacial surface area.

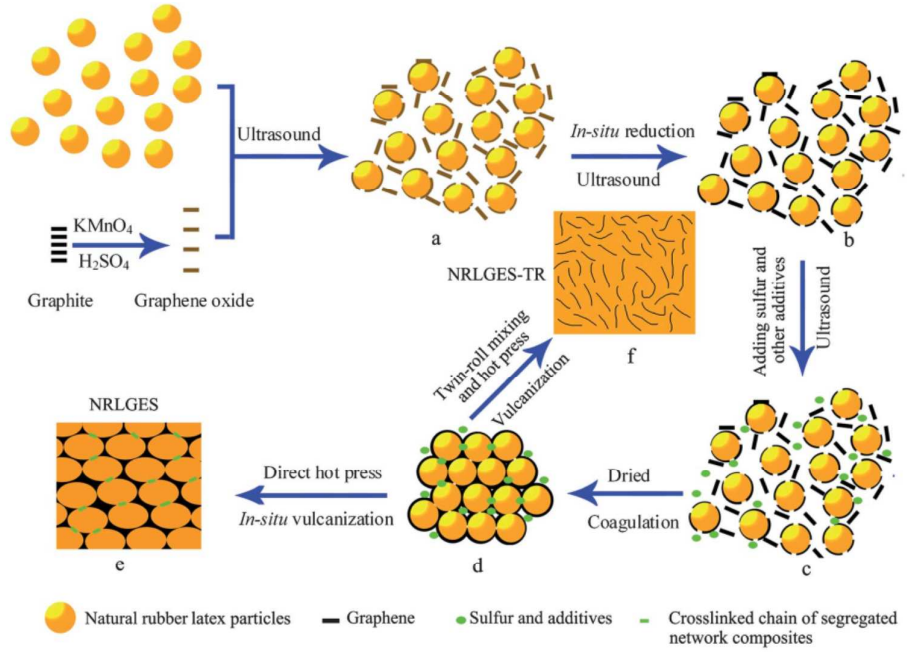

Figure 16. Scheme illustrating the preparation of RGO/rubber composites with a conductive segregated network of RGO by self-assembly in latex and static hot-press. Reproduced from ref. [94] with permission from the Royal Society of Chemistry.

Luo *et al*.[121] proposed a similar electrostatic self-assembly approach by reducing GO in the presence of a cationic polymer poly(diallyldimethylammonium chloride) (PDADMAC), which allowed introducing positive charges on the surface of graphene nanosheets. The positively charged PDADMAC-functionalized graphene was subsequently assembled with negatively charged NR latex particles. Vulcanizing agents were then added and the mixture was freeze-dried and hot molded. As the rubber melt upon cooling, graphene could only be positioned at the surface of the resulting dense packing of micrometer size latex particles. This morphology was confirmed by SEM observations. When the graphene content was over 0.42 vol%, the tensile strength and elongation at break of graphene/NR nanocomposites decreased gradually, which was attributed to the rigid 3D graphene networks that can cause the brittleness and ultimate failure of the composites as stress concentrative points. Thus, high nanofillers loading could lead to processing difficulties and loss of mechanical strength for rubber materials.

Along with NR matrices, some authors have studied other cross-linked systems. In Xing *et al.* work,[122] styrene butadiene rubber (SBR) latex was mixed with aqueous GO suspension prior to co-coagulation using saturated sodium chloride solution to form aqueous suspension of GO-SBR particles that was further reduced using hydrazine. After filtration, the curing agents were added on an open twin-roll mill. Enhanced mechanical properties, low heat buildup, improved wear resistance and thermal stability, as well as good gas impermeability and electricity conductivity were observed. Mao *et al*.[123] fabricated GO/SBR microparticles, in which the GO sheets are trapped in a well-dispersed state throughout the SBR matrix, by combining the latex compounding and spray drying methods. A GO suspension mixed with SBR latex was fed to an air atomizing spray drier. The vast expansion of water molecules during evaporation prevented the GO sheets from aggregating, and the GO sheets were well isolated by the SBR particles. The spray dried GO/SBR powder was collected and mechanically blended with vulcanizing agents on a two-roll mill. A shift in T_g towards higher temperatures was attributed to the exfoliation of GO sheets in the SBR matrix and the strong interface between the rubber molecules and the GO sheets, which lowered the mobility of the molecular chains. By combining latex compounding and spray drying, the reinforcing efficiency of GO was enhanced through the excellent dispersion of GO sheets in the matrix and the strong GO–matrix interface. Tian *et al.*[124] produced composites based on carboxylated nitrile rubber (XNBR) latex particles and GO. A cellular morphology driven by hydrogen bonding interaction between XNBR and GONS during latex mixing was observed. *In situ*

thermal reduction of GO in the GO-XNBR composites was experimented and showed a moderate reduction efficiency. The final composites exhibited low DC conductance but high dielectric constant and low dielectric loss.

Yousefi *et al.*[125] studied GO composite with epoxy matrix by directly mixing a GO suspension with waterborne epoxy system followed with and without a chemical reduction step. After addition of hardener, the mixture was evaporated at 60 °C. The reduction mechanism of GO using hydrazine was studied and it was concluded that the reduction process did not proceed completely. Some nitrogen atoms were immobilized on the RGO surface in the course of reduction. These immobilized nitrogen atoms are highly reactive and could penetrate into epoxy molecules upon the introduction of graphene sheets. In this case, GO sheets act as an intermediary and carry the immobilized nitrogen on their surface, allowing it to react with the epoxy molecules. Through this mechanism, a covalent bond can possibly evolve between the epoxy molecules and RGO sheets upon *in situ* reduction. In addition, with the abundance of aromatic rings in GO, RGO and epoxy, one may expect epoxy and GO interact with each other through non-covalent π–π stacking mechanism. However, a lack of π-π stacking in the composites was observed and is likely due to the hindrance in spatial freedom of epoxy molecules due to the presence of covalently grafted molecules. Addition of GO or RGO into the epoxy matrix improved the Young's modulus, the thermal stability and the tensile strength of the composites, with RGO exhibiting a more pronounced effect.

5. Graphene-based Nanocomposites via *in situ* Polymerization

The *in situ* polymerization route to graphene-based nanocomposites involves the polymerization of hydrophobic monomers in the presence of preformed graphene nanosheets. *In situ* polymerization can be performed in homogeneous conditions (*e.g.*, bulk/solution) or in a heterogeneous environment using one of the four main processes depicted in Section 3. To avoid any ambiguity in the definition of the polymerization type (as sometimes occurs in literature), the present article will use the term "miniemulsion" whenever miniemulsion droplets are formed in the presence of a hydrophobe employing high energy mixing devices (like ultrasonication of high pressure homogenizers), and subsequently polymerized using water- or oil-soluble initiators. The term "suspension" will be used when regular stirrers are employed in combination with organo-soluble initiators.

Contrary to the latex blending strategy in which graphene, GO and RGO are equally applicable, *in situ* polymerization studies almost exclusively employ GO nanosheets due to their surfactant-like behavior.[103, 126,127] Indeed, GO platelets can efficiently stabilize emulsion or miniemulsion droplets, which can be subsequently converted into composite latex particles of similar size through droplet nucleation using either emulsion, suspension or miniemulsion polymerization processes (referred to as Pickering emulsion, Pickering suspension or Pickering miniemulsion polymerizations, respectively).

As an alternative, hydrophobized GO sheets previously dispersed into the monomer phase can be encapsulated by miniemulsion polymerization using molecular surfactants as stabilizers. It has also been shown that composite particles can be formed via conventional soap-free emulsion polymerization even if the original graphene platelets do not have the ability to stabilize the monomer droplets. At last, GO (or graphene) can also be combined with surfactant in conventional emulsion or miniemulsion polymerization processes. Since these approaches can be applied to different polymerization techniques, the sections in this part are structured by polymerization type and contain description of the relevant processes introduced above.

5.1. Emulsion Polymerization

Emulsion polymerization in the presence of GO nanosheets and surfactants

The first report on the synthesis of graphene-based composite materials through conventional emulsion polymerization can likely be attributed to Ding *et al.*[128] Intercalated nanocomposites based on GO and PS were successfully obtained by polymerizing St in the presence of GO at 60°C using potassium persulfate (KPS) as initiator and sodium lauryl sulfate (SLS) as anionic surfactant. Confinement of the polymer chains between the graphene layers was proven by wide angle X-ray diffraction (WAXD), differential scanning calorimetry (DSC) and thermal gravimetric analyses (TGA) which all indicated strong affinity of the polymer for the GO surface and successful intercalation. However, since the latex was coagulated before characterization, no information was given on particle morphology. Following a very similar procedure but with a non-ionic surfactant, Zhang *et al.*[129] reported *in situ* emulsion terpolymerisation of St, *n*-butyl acrylate (BA) and MMA in the presence of GO and a small amount of acrylic acid (AA) as a fourth monomer. TEM, high-resolution electron microscopy (HREM) and WAXD analyses all indicated an exfoliated morphology. Drying of the latex suspension produced films exhibiting enhanced thermal stability and more favorable

flammability properties with only 1wt% of GO (compared to GO-free analogues). The presence of graphite sheets hindered the diffusion of volatile decomposition products within the nanocomposite by promoting char formation, which resulted in a 45% decrease of the heat release rate and a reduction in total smoke production and smoke release rate as demonstrated by cone calorimetry. Unfortunately again, no information was given on particle morphology.

In the same year, Wang *et al.*[130] described the synthesis of similar intercalated PMMA/GO nanocomposites with improved electrical and mechanical properties. More recently, Hu *et al.*[131] reported *in situ* emulsion polymerization of St in the presence of GO and SDS, followed by reduction with hydrazine hydrate to recover electrical properties. TEM showed the formation of PS spheres around 90–150 nm in diameter attached to the edges of the graphene nanosheets (Figure 17a). This morphology was tentatively ascribed to SDS adsorption on the oxygen-containing functional groups present at the sheet edges and subsequent nucleation of the adsorbed micellar aggregates. However, work by Glover *et al.*[132] showing that SDS does not adsorb onto GO sheets (due to electrostatic repulsions between the negatively-charged SDS head groups and the carboxylate groups of oxidized graphene) casts doubt on this proposed nucleation mechanism. GO is however known to contain residual un-oxidized sp^2-hybridized domains[133] onto which SDS may adsorb (as reported by Hsieh *et al*,[134,135]), offering an alternative adsorption theory which might explain the observed morphology. The obtained products were dispersed in toluene (a good solvent for PS) and no precipitation of the GO was observed after 96 hours, suggesting covalent attachment of some polymer chains to the GO surface. The composite material again displayed a significant improvement in thermal behavior compared to the pure polymer, with an increase of the onset of the thermal degradation temperature of 80 °C (Figure 17b) and a significant increase in *Tg* (8°C). A similar improvement in thermal properties was attained in a comparable PMMA/graphene nanocomposite system reported by Kuila *et al.*[129]

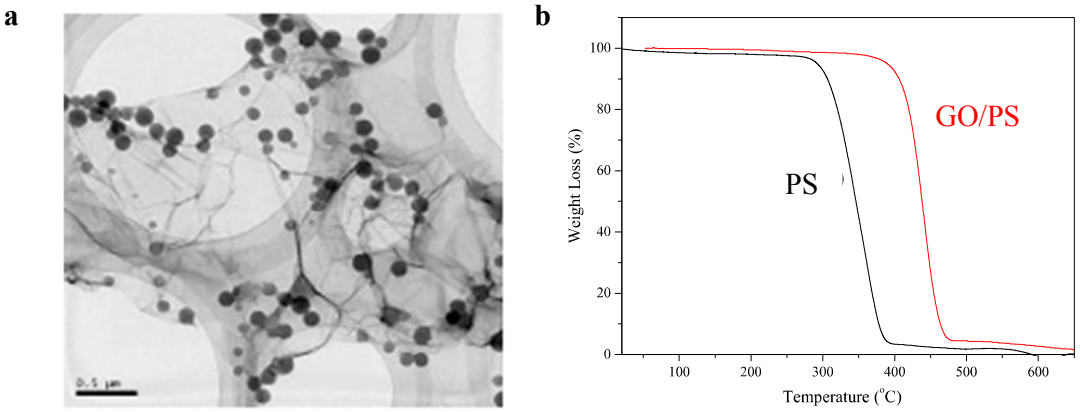

Figure 17. a) TEM image of GO/PS nanocomposites obtained by *in situ* emulsion polymerization showing preferential nucleation of PS particles on the edges of the GO sheets and b) TGA analysis showing an increase of the onset of the thermal degradation temperature of the nanocomposite compared to neat PS. Reproduced from ref. [131] with permission from Elsevier.

The ability to tune the latex particle size by varying the GO content was highlighted by Kattimuttathu *et al.*[136] The hydrodynamic diameter (D_h) of the resulting composite particles decreased from 292 nm to 88 nm with increasing GO content from 0.1 wt% to 1 wt% (based on monomer), and was significantly smaller than that of the blank latex (D_h = 539 nm) synthesized under the same conditions in the absence of GO. Although this article indisputably showed an effect of GO on the final latex particle size, atomic force microscopy (AFM), SEM and TEM did not clearly support the authors' claims of the presence of the GO sheets at the particle surface, instead showing smooth elongated monodisperse latex particles without clear evidence of GO sheets being located there. Indeed, the latter had an average size of 280 ± 30 nm as determined by dynamic light scattering (DLS), whose size was of the same order of magnitude or larger than the latex particles size. Unless those large sheets were capable of wrapping around the latex particles (which seems unlikely for the very small particles), they should have been visible in the TEM images either as latex-decorated GO sheets or as rough latex particles. The fact that we cannot see them despite their potential to decrease the final particles size raises serious question about the exact mechanism of particle formation, considering in particular that surfactant was also used in conjunction with GO.

Emulsion polymerization in the presence of GO nanosheets as the sole stabilizer

Apart from the combined use of GO and surfactants in conventional emulsion polymerization, there are also a few reports in which GO was used as the sole "surfactant". The first example of graphene-based colloidal nanocomposites involving graphene as the sole stabilizer was reported by Thickett *et al.*[137] who used exfoliated GO sheets with lateral dimensions of approximately 200 nm to form graphene-armored latex particles through conventional surfactant-free emulsion polymerization of St using KPS as thermal initiator. The nanosheets were obtained by a modified Hummer's method (see Section 2.1), and was used at concentrations above a certain threshold in order to efficiently stabilize the latex particles. TEM images revealed rough particle surfaces indicating the presence of adsorbed GO sheets (Figure 18a). Interestingly, the presence of just 0.11 wt% GO (relative to St) decreased the particle size from 850 nm in the GO-free system to 259 nm. However, the system then behaved unexpectedly for higher GO contents or for higher initiator concentrations, with the formation of micron-sized aggregates of GO sheets and polymer latex particles (Figure 18b). This intriguing result was attributed to GO instability at high ionic strength (as an increase in GO content itself or in the initiator concentration both constitute an increase of ionic strength). A certain minimum ionic strength was required to create "unstable" precursor particles and promote heterocoagulation between the destabilized GO sheets and the growing oligomers, but too high an ionic strength led to GO destabilization and ill-defined morphologies. In addition to demonstrating good stabilizing properties, GO was also shown to behave as a radical inhibitor resulting in limiting conversions. This is consistent with the high concentration of phenolic hydroxyls in the GO structure, which are known to be efficient radical scavengers as mentioned earlier in Section 2.4.

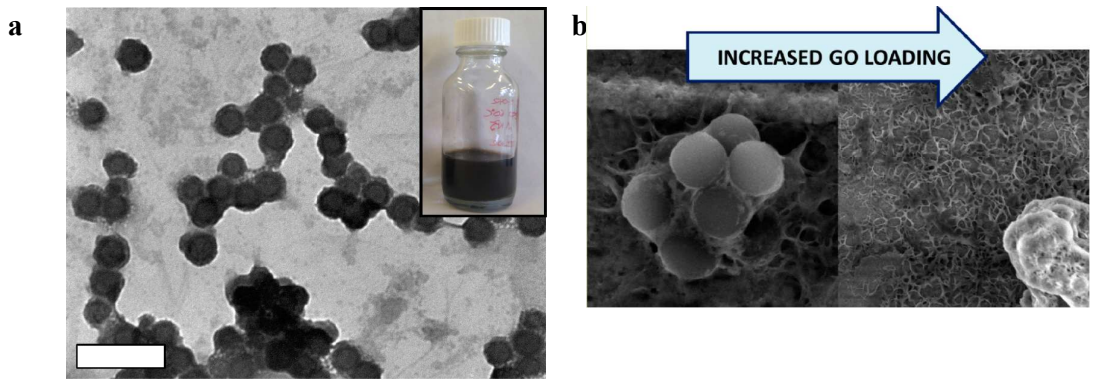

Figure 18. a) TEM image of GO-armored PS particles obtained via emulsion polymerization of St in the presence of 1 wt% of GO (relative to monomer) at low initiator concentration

([KPS] = 2 mM), and b) Morphological change observed upon increasing GO loading. Reproduced from ref. [137] with permission from the American Chemical Society.

In the same period, Yin *et al.*[138] also reported the successful formation of GO-coated PS particles using GO platelets with lateral dimensions between 400 nm and 1 μm through surfactant-free emulsion polymerization. Since the GO platelets did not have the ability to stabilize the emulsion droplets, the polymerization should be regarded more as a polymerization performed in the presence of GO platelets than as a true "Pickering" emulsion polymerization. The resulting PS microspheres were nevertheless covered with wrinkled GO sheets indicating high affinity of GO for the latex particles. It was proposed that the PS oligomers formed in the early stages of the polymerization adsorbed on the GO surface through π–π interactions, which was confirmed by Fourier-transform infrared (FTIR), WAXD and TGA analyses. The presence of adsorbed PS chains promoted subsequent heterocoagulation of the hydrophobized GO sheets with themselves or with primary latex particles, resulting in the formation of armored latexes whose stability was ensured by the negatively-charged GO. Although the GO content was significantly higher than in the earlier work by Thickett *et al.*[137], the authors did not report any stability issues as long as the pH value was sufficiently high (i.e., above 4) to ensure sufficient electrostatic repulsions. It is noteworthy that Thickett *et al.* did not indicate the pH value, which may therefore have contributed to the intriguing results, which were observed at higher GO contents.

With the aim of producing exfoliated PS/GO nanocomposites, Yeole *et al.*[139] recently developed a method based on the combined used of reversible addition fragmentation chain transfer (RAFT) polymerization and surfactant-free emulsion polymerization. The carboxyl-bearing RAFT agent dodecyl isobutyric acid trithiocarbonate (DIBTC) was first attached to the GO sheets via esterification with the surface hydroxyl groups. The resulting RAFT-functionalized GO particles were then used as seeds in soap-free emulsion polymerization of St using KPS as initiator and styrene sodium sulfonate (SSNa) as auxiliary comonomer. The use of an auxiliary comonomer has often been reported in the literature as an efficient mean to promote the adhesion of solid particles to the surface of latex particles in soap-free emulsion polymerization processes stabilized by inorganic particles.[77-79] Although GO is technically not an inorganic compound, SSNa likely played a similar role here: increasing the affinity of the growing oligoradicals for the GO surface via π□□□□□□□□□□□n□□□□□□□□□□, thus allowing the polymerization to effectively take place on the sheets surface. In the present

example, the anchored RAFT agent also played an important role in promoting polymerization from the GO surface.

Pickering emulsion polymerization

There is to our knowledge only one report that falls into the category of Pickering emulsion polymerization.[140] In this example, St droplets were emulsified in the presence of small GO sheets as the sole stabilizer (with lateral dimensions around 200 nm) and subsequently polymerized at 25°C using KPS and sodium thiosulfate ($Na_2S_2O_3$) as redox initiator. The emulsion stability was strongly influenced by pH, with unstable emulsions obtained for low (< 2) or high (> 9) pH values, respectively. Subsequent polymerization of the Pickering emulsion generated large PS particles with a wrinkled surface texture, which was attributed to phase separation between GO and PS (Figure 19). Even though this has not been raised in the article, incomplete monomer conversion and residual monomer evaporation during sample preparation may have also contributed to the observed morphology.

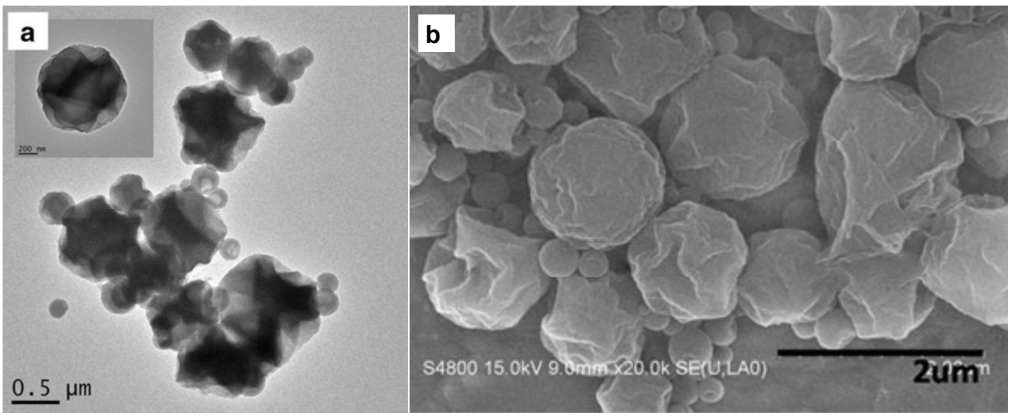

Figure 19. a) TEM and b) SEM images of PS/GO composite particles synthesized by Pickering emulsion polymerization at pH 3 using KPS/$Na_2S_2O_5$ as redox initiator. Reproduced from ref. [140] with permission from Springer.

Emulsion polymerization in the presence of graphene

Due to its absence of surface charge, graphene is less suited than GO for the generation of hybrid latexes since interaction with the latex particle surface is more difficult. Despite this, Hassan *et al.*[141] reported the synthesis of graphene comprised of a few layers from thermally expanded graphite, and its subsequent use in emulsion polymerization. The expanded graphite was exfoliated in an SDS solution by ultrasonic treatment resulting in FLG with on average

3–10 layers and relatively few defects. *In situ* emulsion polymerization of St was performed at 70 °C using KPS as initiator, sodium hydrogen carbonate as buffer and SDS as additional surfactant. The resulting composite material was characterized by TEM showing the presence of PS latex particles decorating the surface of the large graphene sheets, but the colloidal stability of the resulting hybrid suspension was not stated.

5.2. Miniemulsion Polymerization

A substantial number of studies have employed GO platelets in miniemulsion polymerization systems, and can be classified into three categories. The first category comprises of GO-armored latexes in which a species other than GO is used as stabilizer. The second category comprises of GO-armored latexes in which GO acts as the sole stabilizer. In this case, miniemulsion droplets are formed by adding the monomer to an aqueous dispersion of GO and applying ultrasound to the resulting suspension. The stability of the droplets is maintained by the presence of the GO sheets and by the use of a hydrophobic species that suppresses the molecular diffusion between droplets. Ideally, each droplet is then nucleated to produce a 1 to 1 particle copy, thereby forming the graphene-armored latex. The third category is GO-encapsulated latexes, in which miniemulsion polymerization is exploited to physically entrap GO inside polymer particles. Using miniemulsion polymerization for this purpose is simpler than employing a conventional emulsion approach since it avoids the often-complicated nucleation step. All these strategies are described in the following paragraphs.

Miniemulsion polymerization using GO together with surfactants

Although less common than Pickering systems, miniemulsion polymerizations have sometimes been conducted in the presence of both GO and surfactant.[142,143] In these examples, the GO sheets do not participate in the stabilization of the miniemulsion droplets, with the surfactant instead performing this function. Following this approach, Etmimi *et al.*[143] prepared P(St-*co*-BA)/GO nanocomposite latexes containing exfoliated GO nanosheets. TEM showed the formation of 80–200 nm latex particles connected to one another by the GO platelets (which appeared as dark lines in the images). This morphology is on the whole similar to that reported above in conventional emulsion polymerization.[131] The strategy was extended by the same team by treating the nanocomposite suspension with hydrazine hydrate to reduce the functional groups of GO.[144] The presence of the surfactant maintained a stable suspension that

could be processed into a composite film exhibiting enhanced water barrier properties compared to the neat polymer film and to the same film loaded with GO platelets.

Pickering miniemulsion polymerization

The first use of a true Pickering miniemulsion polymerization process for the synthesis of latex particles armored with nanosized GO sheets was reported by Che-Man *et al*.[145] in 2013. Relying on the ability of GO nanoplatelets to act as a surfactant in mixtures of hydrophobic liquids and water,[103,146,147] the authors described the formation of St miniemulsion droplets stabilized by GO sheets using HD as hydrophobe. A mixture of monomer, GO suspension (with GO sheets of different size), initiator (AIBN) and HD was sonicated 10 minutes before polymerization. The nanoscale GO sheets were prepared from graphite nanofibers of diameter approximately 100 nm, thus ensuring the absence of very large sheets. Varying the ultrasonication time during the exfoliation step enabled control over the final sheet diameter, which varied from 20 to 180 nm as estimated by DLS. Three different sheet sizes were tested at increasing loadings (1 to 5 wt%) for their ability to stabilize the miniemulsion at 10 wt% monomer content. Only the small GO sheets at the highest loading allowed efficient stabilization. Fixing this ratio between GO and monomer, the stability of systems containing different monomer contents was then tested. The miniemulsion with intermediate monomer content of 7.5 wt% exhibited superior stability compared to smaller (5 wt%) or higher (10 wt%) contents. As the ratio of GO to St remained constant, this result was tentatively attributed to insufficient amounts of GO sheets to cover the total droplets surface area for low monomer contents, and to the presence of free GO sheets located in the aqueous phase for too high concentrations, which would decrease droplet stability. TEM, SEM and DLS all indicated the formation of large PS beads coated with GO sheets with a broad particle size distribution (PSD). Their diameters increased from approximately 150 to 460 nm with increasing monomer conversions (Figure 20), suggesting progressive particle aggregation due to limited miniemulsion stability. Crumpled particles of highly irregular and nonspherical shape were obtained at low conversions due to the evaporation of unreacted styrene during sample preparation. This is consistent with the droplet nucleation mechanism of miniemulsion systems. Interestingly, GO underwent a partial reduction during the polymerization (shown by zeta potential measurements, X-ray photoelectron (XPS) and FTIR spectrocopies), which may also explain the decrease in stability of the miniemulsion over time.

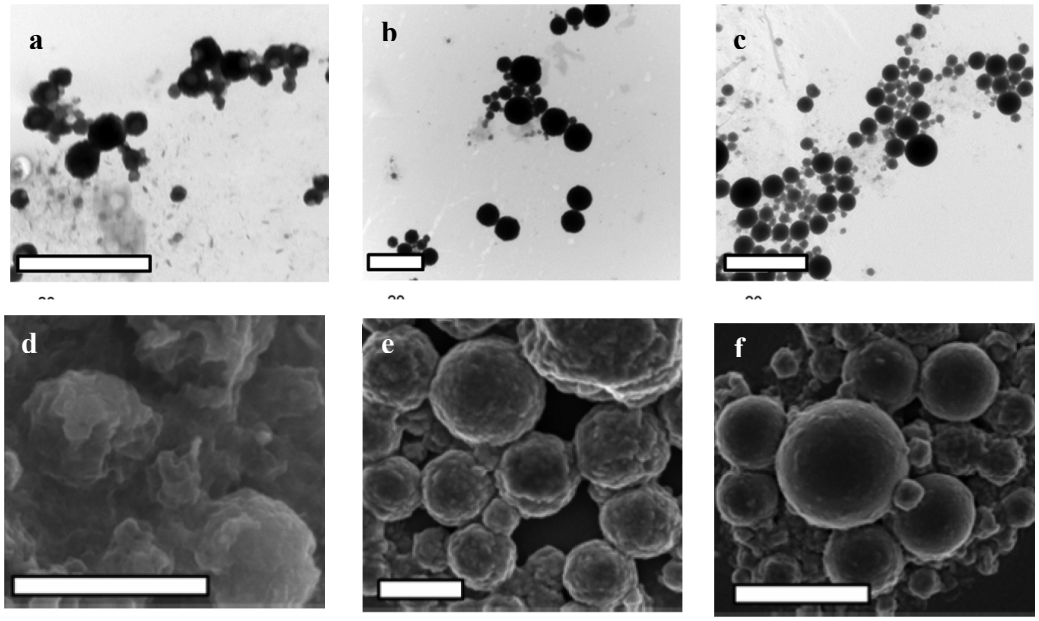

Figure 20. Top: TEM and bottom: SEM images of polymer/GO composite particles obtained at 19% (a and d), 47% (b and e) and 90% (c and f) of monomer conversion during Pickering miniemulsion polymerization of St using GO as solid stabilizer. Scale bars: 2 μm for a, b, c and f and 500 nm for d and e. Reproduced from ref. [145] with permission from Wiley Periodicals.

The influence of various parameters such as monomer polarity, pH value and ionic strength on the miniemulsion stability and composite particle size was subsequently studied in more detail.[148,149] Apolar monomers such as lauryl methacrylate, benzyl methacrylate and St allowed the formation of more stable miniemulsions compared with more polar monomers. These could be successfully polymerized without significant formation of coagulum and/or phase separation, giving particles with diameters in the range 200–1000 nm with rough surface morphologies.[148] The amphiphilicity of GO could also be tuned by adjusting the pH value or the ionic strength of the aqueous solution. While pH had only a minor effect on miniemulsion stability and final particle size, increasing ionic strength compressed the electrical double layer, which made the GO sheets more hydrophobic. This promoted their adsorption at the oil/water interface resulting in better colloidal stability.[149]

Very recently, the Pickering miniemulsion polymerization technique was taken a step further to generate hollow hybrid capsules consisting of a cross-linked polymer shell and a GO coating.[150] In this work, micron-sized droplets stabilized by nanometric GO platelets (with lateral dimensions of around 30 nm) were generated by ultrasonication using St as monomer,

HD as inert liquid core material, divinylbenzene (DVB) as cross-linking comonomer and AIBN as initiator. The droplets were subsequently polymerized at 70 °C (strategy depicted in Figure 21a). The role of the HD was to act as a "templating" liquid for the nanocapsule formation. In this commonly applied strategy for obtaining nanocapsules, the polymerization of the monomer(s) commences at the droplet surface and proceeds inwards. After complete monomer consumption, the templating liquid (which is present at much higher concentration than those used for hydrophobes in normal miniemulsion systems) remains in the particle core and can be removed to furnish the hollow particles. In this example, remarkably stable and robust hollow capsules (the capsules could withstand multiple centrifugation/steps without collapsing) with an exceptionally thin shell, were obtained at an HD load of around 50 % w/w (Figure 21b) whereas lower loadings generated porous particles. Interestingly, the suspension remained colloidally stable after chemical reduction with hydrazine hydrate, suggesting that some oxidized groups were retained on the GO surface (*i.e.*, incomplete reduction). This hypothesis was indeed confirmed by zeta potential measurements, which showed that the particles retained a strong negative charge (ZP = -40 mV).

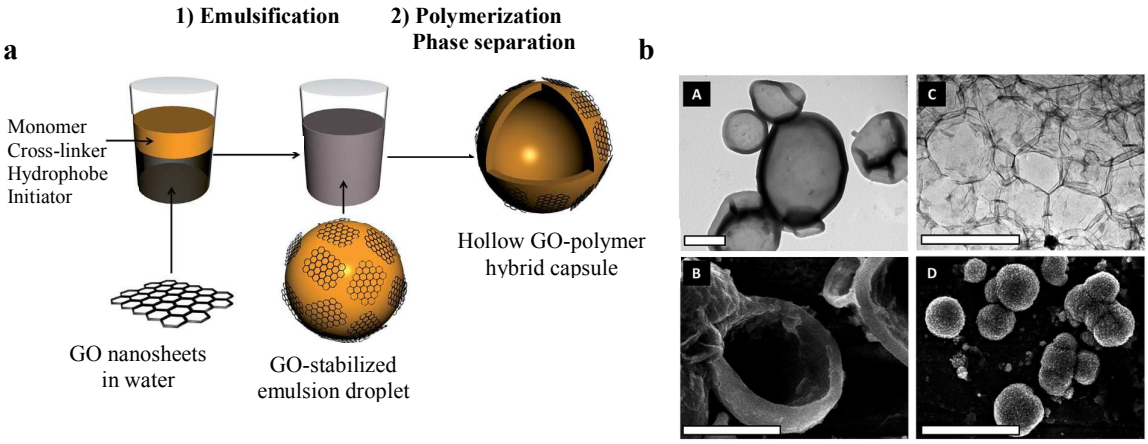

Figure 21. a) Scheme illustrating the procedure used to create hollow GO-polymer hybrid capsules via Pickering miniemulsion polymerization and b) TEM (top) and SEM (bottom) images of the hollow capsules (scale bars= 1 μm). Reproduced from ref. [150] with permission from the Royal Society of Chemistry.

GO encapsulation by miniemulsion polymerization

The encapsulation of GO within latexes is achieved by functionalizing the GO surface to make it more compatible with the monomer phase. The "compatibilized" GO then

preferentially resides inside the monomer droplets rather than at their surface. If compatibilization is performed using a species that is capable of controlling the subsequent polymerization, such as a surface-bound RAFT agent, the added benefit of molar mass control can in addition be imparted to the polymer latex.

With the aim of encapsulating GO sheets in polymeric particles, Etmimi *et al.*[151] reported the synthesis of polystyrene/GO nanocomposites via RAFT polymerization in miniemulsion. GO modification was carried out via esterification of the surface hydroxyl groups with dodecyl isobutyric acid trithiocarbonate (DIBTC). The RAFT agent-grafted GO was dispersed in water, mixed with the oil phase composed of the monomer (St), the initiator (AIBN) and the hydrophobe (hexadecane, HD) and sonicated to allow effective swelling of the GO platelets with St. The oily phase was then diluted with an aqueous solution of SDBS, and sonicated further to form a miniemulsion before polymerizing at 75°C. TEM showed the formation of stable monodisperse PS/GO composite latexes with encapsulated GO sheets. SEC analysis of the PS chains after cleavage from the GO surface showed a good control of the polymerization ($Đ$ ranging from 1.6 to 1.2), with better control attained at the highest GO (and therefore RAFT agent) content. The resulting polymer/GO nanocomposites presented enhanced mechanical and thermal properties compared to the neat polymer.

In a related study conducted by the same research group,[152] P(St-co-BA)/GO nanocomposites were prepared using 2-acrylamido-2-methyl-1-propanesulfonic acid (AMPS)-functionalized GO sheets. The GO sheets were dispersed in the monomer phase and the mixture was (mini)emulsified using SDS as surfactant and HD as hydrophobic co-stabilizer. Comparing the results obtained under the same conditions but using un-modified GO sheets, the authors showed that only the AMPS-functionalized GO sheets could be successfully encapsulated (Figure 22).

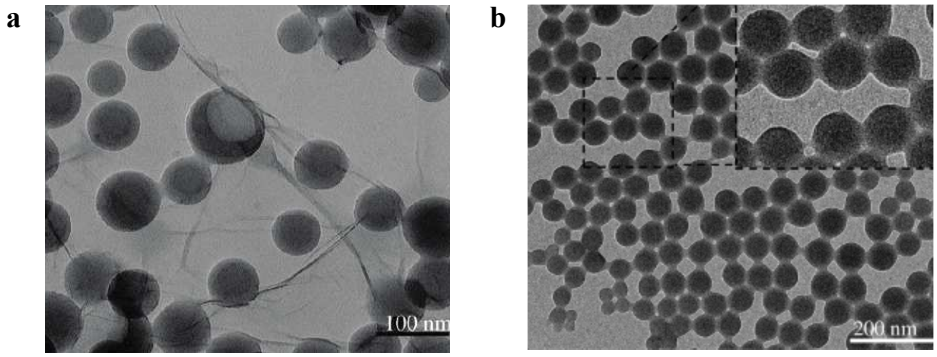

Figure 22. TEM images of P(St-*co*-BA)/GO nanocomposite latexes made by miniemulsion polymerization with 1 wt% (relative to monomer) of a) unmodified GO and b) AMPS-modified GO. The left image shows that most of the GO sheets have not been encapsulated by the copolymer shell whereas the AMPS-functionalized GO sheets have been successfully encapsulated. Reproduced from ref. [152] with permission from the American Chemical Society.

5.3. Suspension Polymerization

Similarly to miniemulsion polymerization, in suspension polymerization, each monomer droplet can be considered to be a batch reactor. Suspension polymerization differs however from miniemulsion polymerization in the size and stability of the monomer droplets. Miniemulsion polymerization takes place in relatively small, submicrometer-size droplets, whereas suspension polymerization occurs in significantly larger (typically from 1 μm to 1 mm diameter) droplets. In suspension polymerization, droplets are generally stabilized against coalescence using water-soluble polymeric stabilizers (often referred to as protective colloids) or colloidal inorganic powders used as Pickering dispersants. The utilization of graphene sheets as solid stabilizers appears therefore quite natural in this case.

Several authors have reported the free radical polymerization of coarse emulsion droplets stabilized by GO sheets using AIBN as initiator.[153,154,155,156] In these examples, the mixture of monomer, GO suspension and AIBN was emulsified using ultrasound to promote GO exfoliation and create emulsion droplets which were subsequently polymerized. Although droplets were small (< 1 micron) and were dispersed by ultrasonication (typical of Pickering miniemulsion polymerization), the absence of added Ostwald ripening retardant meant that droplet coalescence was not prevented. This process is therefore more appropriately defined as a Pickering suspension-like polymerization process. Both PMMA/GO[153] and PS/GO[154,155,156] composites were synthesized by this approach. In the case of PMMA, it was found that a minimum concentration of GO (*i.e.*, typically 4 wt% based on monomer) was necessary to stabilize the monomer/water interface, and hence the resulting polymer particles (Figure 23). Indeed, unstable latexes were obtained for lower concentrations. The final composite polymer particles displayed a broad size distribution (with diameters ranging from 0.1 and 0.8 μm) as expected for suspension polymerization. The GO sheets also had a broad lateral size distribution, resulting in various hybrid morphologies as shown in Figure 23. While large GO sheets could wrap individual latex particles resulting in a partial coverage (Figure 23b), smaller sheets formed an armored morphology with a rough texture (Figure 23a). Very large

sheets with lateral dimensions higher than the latex diameter could stabilize two or more particles simultaneously (Figures 23c and 23d). Similar results were obtained for the PS/GO nanocomposites.

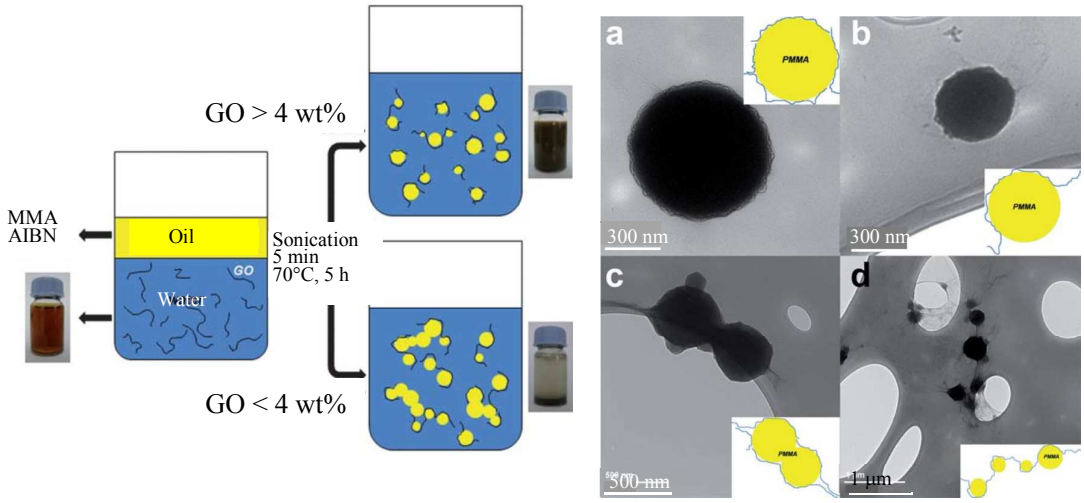

Figure 23. Left: Scheme illustrating the Pickering suspension-like polymerization process used to synthesize PMMA/GO composite particles, and right: TEM micrographs showing various arrangements of the GO sheets at the polymer particles surface depending on their lateral dimensions. Reproduced from ref. [153] with permission from the Royal Society of Chemistry.

In a related work which applied vigorous agitation at 2000 rpm instead of ultrasound to disperse the droplets, Dao *et al.*[157] reported the successful formation of graphene-coated PMMA latex particles through Pickering suspension polymerization. Graphene was rendered water-dispersible by reaction of its epoxy groups with potassium 2-aminoethanesulfonate. The resulting aqueous dispersion was then mixed with MMA containing AIBN to form graphene-stabilized monomer droplets under vigorous agitation, which were subsequently polymerized at 70 °C. SEM showed the formation of rough particles tightly wrapped in the sulfonated graphene sheets. Their diameter decreased from around 220 nm to 60 nm with increasing graphene content, highlighting the high stabilizing efficiency of the surface-modified graphene.

5.4. Other Related Approaches

There are in the recent literature a few systems that do not follow any of the procedures described so far. These are microemulsion and precipitation polymerization systems. The principles of precipitation polymerization have been described in section 3.4 and will not be repeated here. As regards microemulsion polymerization, it begins in a thermodynamically stable emulsion of nanometer-size droplets spontaneously formed in the presence of high concentrations of surfactants. It thus does not require the high shear conditions generally applied in the formation of (mini)emulsion or suspension droplets and allows the elaboration of very small (in the order 5-50 nm) polymer particles.

Patole *et al.*[158] carried out *in situ* microemulsion polymerization of St in the presence of thermally expanded graphene (EG) using AIBN as initiator, SDS as surfactant and 1-pentanol as co-stabilizer. Thermally expanded graphene consisting of 1-10 layers of graphene with micrometric lateral dimensions was first sonicated in the presence of SDS and 1-pentanol. The monomer and the initiator were next introduced into the graphene dispersion and the mixture was sonicated for an additional 4 hours at 0 °C before starting polymerization at 85 °C (Figure 24a). Electron microscopy analyses (TEM and SEM) showed the presence of anchored PS particles on both sides of the graphene sheets (Figures 24b and 24c). It was argued that the SDS-stabilized microemulsion droplets underwent frequent collisions with the graphene flakes, promoting anchoring of the PS particles on the sheet surface and displacement of the SDS molecules at the contact region. Charge repulsions between the hydrophilic ends of SDS adsorbed on both the graphene sheets and the monomer droplets were overcome by the kinetic energy of Brownian motion of both species, resulting in reversible interactions. The resulting PS/graphene nanocomposites formed conductive films with high flexibility. In a subsequent work,[159] the graphene sheets were combined with CNTs with the aim of further improving the mechanical properties of the composite materials by forming an interconnected nanocomposite network in which the nanotubes bridged the gap between the large graphene sheets.

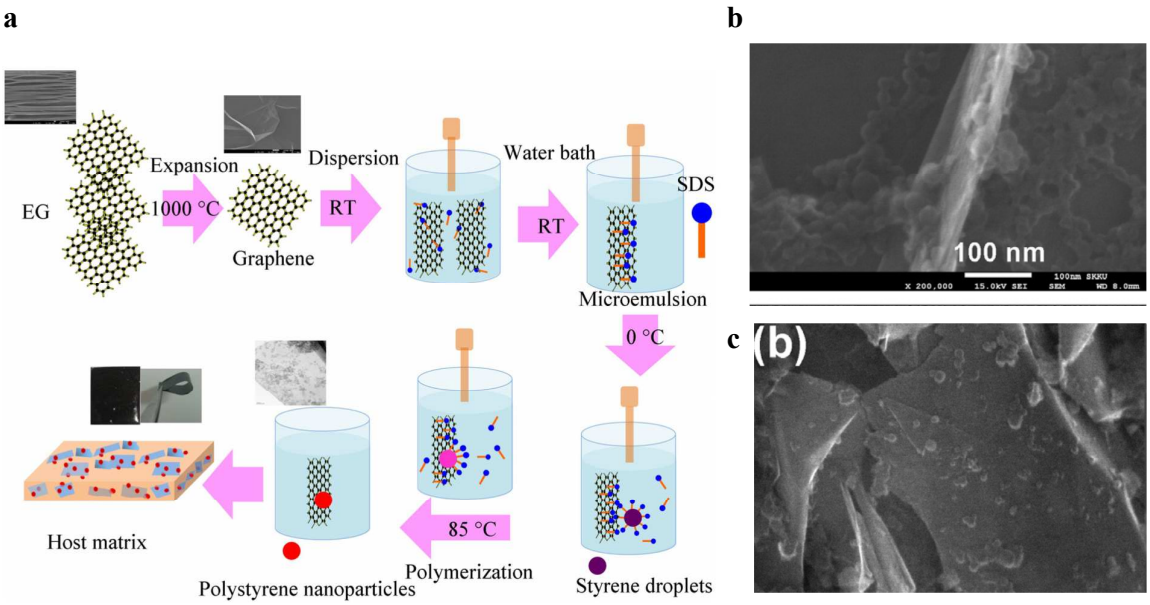

Figure 24. a) Scheme illustrating the multi-step process used to form PS/graphene nanocomposites by *in situ* microemulsion polymerization and b, c) SEM and TEM images of the resulting composite particles showing the formation of PS latexes on the surface of the graphene flakes. Reproduced from ref. [158] with permission from Elsevier.

Applying a precipitation polymerization process in a water/methanol mixture, Thomassin *et al.*[160] formed PMMA/GO nanocomposites. The amphiphilic properties of the GO sheets drove them to the interface of the PMMA particles during the polymerization reaction, leading to the formation of an armored morphology as attested by TEM and SEM. It was argued that this morphology was favored by *in situ* grafting of PMMA chains to GO resulting in enhanced hydrophobicity. The average particle size decreased with increasing GO content, providing additional evidence that the sheets participated in latex stabilization. After drying and compression molding, the GO sheets formed a regular honeycomb pattern within the polymer matrix.

6. Properties of Graphene-Latex Nanocomposites

The primary goal of incorporating inorganic materials into polymer latexes is to improve the performance of the resulting materials. Even low inorganic contents can impart marked improvements in material properties, such as greater mechanical strength and durability, lower liquid and gas permeability, and electrical conductivity. The following section will

describe the functional properties of materials formed from graphene-based nanocomposite latexes. The influence of physical properties and morphology of the precursor hybrid latexes will be emphasized. In their review focusing on graphene-based nanocomposites (not specifically latex-based), Potts *et al.*[6g] reported the rheological, electrical, mechanical, thermal, and barrier properties of these materials, and how each of their properties is dependent upon the intrinsic properties of graphene and graphene-related compounds and their state of dispersion in the matrix. Trends that are observed in generic graphene-based nanocomposites are naturally also observed in graphene-latex nanocomposites. The following section will focus on the specific advantages and challenges of graphene-latex nanocomposites for material applications. Fabrication of composites through the latex route has been widely used in clay-polymer composites for mechanical enhancement for high durability coatings for instance and gas barrier for packaging applications and graphenic fillers are good candidates to fulfill similar property enhancements.

6.1. Mechanical Properties

Jiang *et al.*[98] showed that graphene acts as the primary load-bearing component in graphene-polymer composites, which enhances mechanical properties such as hardness, tensile modulus and yield strength. Several authors have reported increases in tensile modulus with increasing graphenic filler content both in thermoplastic[89,104,112] and cross-linked[94,120,121,125] matrices. Contrary to clay fillers, graphenic fillers are flexible sheets that commonly adopt wavy or wrinkled morphologies[91] once dispersed in a polymer matrix, which may effectively reduce modulus values as crumpled platelets would tend to unfold rather than stretch in-plane under an applied tensile stress.

In rubbery systems, the addition of fillers also modifies the overall mechanical properties which can be considered as a positive or a negative effect depending on the targeted application. Indeed, while addition of filler induces an increase of tensile modulus, it can also induce a decrease of tensile strength and elongation at break. For instance, Luo *et al.*[121] observed that when graphene content is over 0.42 vol.%, the tensile strength and elongation at break of graphene/NR nanocomposites decrease gradually. This was ascribed to the rigid 3D graphene networks that serve as non-elastic reinforcement (stress concentrative points) causing the brittleness and ultimate failure of the composites. Additionally, they also reported that high nanofiller loadings could lead to processing difficulties in that the inferior molecular

contact between vulcanization agents and NR chains - a consequence of the low blending temperature - may affect the cross-linking of NR, thus reducing the mechanical strength.

6.2. Barrier Properties

The incorporation of graphene and GO-derived fillers can significantly reduce gas permeation through a polymer composite compared to the neat matrix polymer.[129] The lower permeation can be attributed to the lamellar structure of the fillers, which creates a 'tortuous path' for diffusing species, thus inhibiting molecular diffusion through the matrix. The chemical nature of the graphene-based filler also has an important influence on the extent to which different molecules are denied passage through the material. Matos *et al*.[92] performed swelling experiments with RGO-rubber and GO-rubber composites and pure rubber in three solvents with different polarities. All the nanocomposite samples absorb less solvent than the pure rubber. The RGO composite swelled more than the GO composite in xylene, while the behavior in water was the opposite. In isopropyl alcohol (intermediate polarity), the two types of composites behaved similarly. The more polar GO is highly suitable for preventing the permeation of apolar species, whereas the less polar RGO filler is more effective in blocking diffusion of polar molecules. Permeability can therefore be tuned for specific applications by controlling the level of reduction of the GO sheets, since this determines the GO/RGO ratio.

6.3. Electrical Conductivity Properties

As more graphene filler is added to a polymer matrix, the composite transitions from insulator to conductor due to the formation of an interconnected graphene network which is intrinsically conductive. The electrical conductivity of graphenic nanocomposites has raised particular interest for applications such as electrostatic discharge and EMI shielding protection, gas sensors and fuel cells. The development of flexible electronic devices has led to a demand for coatings with tailored electrical and functional properties. For these applications, the challenge is to reach the highest conductivity at lowest graphene content so that desirable mechanical properties such as flexibility are not reduced.

A model referred to as the "percolation theory"[161] is very helpful for describing the properties of graphene-latex composites, particularly for understanding electrical properties.[162] The percolation threshold is defined as the theoretical graphene fraction needed to obtain the first continuous graphene path through the polymer matrix. Conductivity undergoes an abrupt

increase at this graphene content, and conductivity can therefore be used to define the percolation threshold.

Below the percolation threshold, the fillers embedded in the composite form "finite clusters" (since they are not completely interconnected), and at or above the percolation threshold they form "infinite" or "percolating clusters." Percolating clusters comprise of a continuously connected backbone decorated with dangling side branches of graphene. As expected, only the backbone carries current when a voltage is applied, since the side branches do not form a continuous path. The percolation threshold can also be estimated by mechanical means, but these methods less accurate since the mechanical response is also influenced by the graphene branches (rather than just the continuous backbone). Moreover, considering that a smaller filler-filler distance is required for electrical conductivity (ca. 5 nm for tunneling effect) as compared to that required to impede polymer mobility (few tens nm for mechanical bridging through the interphase), the percolation threshold for electrical conductivity should be slightly higher than for mechanical percolation.[163,164,165] Noël *et al.*[162] compared the influence of graphene on mechanical and electrical properties in graphene-based composites elaborated through latex blending. It was found that the percolation threshold determined through the analysis of conductivity properties was of same order of magnitude but more precise than the percolation threshold determined through the analysis of mechanical reinforcement.

Several parameters can influence the conductive properties of graphene-latex composites.[6g] The most critical parameters are dimensional parameters such as the aspect ratio (and aggregation) of the graphene[166,167] (with a higher aspect ratio leading to a higher conductivity) and the latex-graphene relative dimensions.[162,168,169] For the latter parameter, the number of possible percolating paths decreases with increasing latex diameter, thus a lower percolation threshold is expected for larger latex beads. Moriarty *et al.*[168] verified this effect using carbon black (CB)-filled composites. Monodisperse copolymer latex particles, each with a different particle size, were prepared. The percolation threshold decreased from 2.7 to 1.1 vol % CB as the polymer particle size increased.

The choice of polymer can also influence the conductive properties. Kim *et al.*[170] studied the mechanical and electrical behaviors of carbon black-latex composites prepared at room temperature from polymer matrices exhibiting different Tgs. Composites made using polymers with higher room temperature modulus (due to higher Tg) exhibited a lower percolation threshold and higher electrical conductivity. When the modulus of the polymer is high, the latex particles tend to maintain their original shape during the coalescence process. In this case, carbon black particles are more effectively forced into the interstitial space

between the polymer particles to form a continuous network at lower concentration. In contrast, lower modulus polymer particles are easily deformed around CB particles, effectively separating them from one another.

The quality and orientation of the graphene nanosheets are other factors impacting the electrical properties. Wrinkled, folded, or otherwise non-ideal platelet conformations can raise the electrical percolation threshold[171] in addition to the presence of isolating polymer or other molecules covering the fillers. Alignment of the filler plays a major role in the onset of electrical percolation: when the platelets are aligned in the matrix, the percolation threshold decreases significantly in the direction of the alignment (in plane) compared with the perpendicular direction. Yousefi *et al.*[100] showed that the conductivities of the latex-based composites containing 0.5 wt% RGO were almost identical in the in-plane and perpendicular directions, showcasing an isotropic behavior and confirming homogeneous and random dispersions of RGO. With higher graphene contents of 2 and 5 wt%, however, conductivity in the in-plane direct increased to several orders of magnitude higher than in the perpendicular direction. The significant anisotropy in electrical conductivity in composites with high RGO contents is associated with the alignment of graphene sheets so that conductive networks are preferentially formed along the plane direction whereas fewer conductive paths are present through the thickness. This suggests the existence of self-alignment in composites of over 2 wt% graphene.

All these parameters can be used to optimize the conductive properties of the final composites. In antistatic coatings applications for example, the minimum required conductivity lies around 10^{-2} S m^{-1} while for conductive inks for electronics, the targeted conductivities are 10–10^{4} S m^{-1}.

Despite this ability to tune conductivities, one question remained outstanding until recently: is it possible to determine the maximum conductivity reachable in graphene-latex composites? To address this question, Ghislandi *et al.*[108] produced graphene powder compacts using compression molding, and graphene paper films through filtration on a polyamide membrane.

The amount of effective charge carriers (graphene fillers) contributing to the overall conductivity is much lower for composites than for powder compacts or paper film due to the much lower filler content in the same corresponding volume. In order to compare the conductivity levels reached in composites to conductivity levels reached in compacts and paper films, the "effective density" of the composite materials has been defined by multiplying the volume fraction of the filler (vol.%) by its density. Figure 25 gathers conductivity versus effective density data for 35 papers comprised of graphene-latex

composites: 24 produced through physical blends and 11 synthesized via *in situ* polymerization. The dimensional characteristics of the composites are given in the right side of the Figure. The latex diameters ranged from few tens of nanometers to a few microns, but were mainly around a few hundred nanometers. The graphene lateral size ranged from a few tens of nanometers to several microns. Finally, it is worth noticing that in most studies the graphene lateral size was larger than the latex diameter.

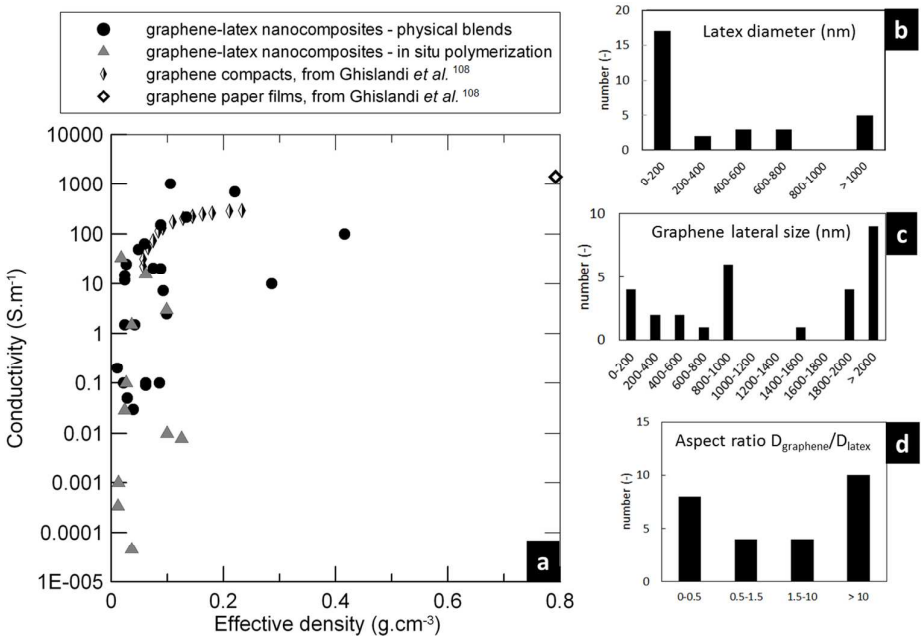

Figure 25. a) Conductivity measurements versus effective density for graphene-latex composites, graphene compacts and paper films, and b, c, d) dimensional characteristics of the 35 composites that were used to generate Figure 25a. Adapted from ref. [108] and supplemented by literature data with permission from Elsevier.

As expected, conductivities matching that of pure particles (10^7-10^8 S m^{-1} for graphene[172]) were not reached in composites, due to inevitable filler-filler contact resistance. For most composites, the conductivity level is adequate for applications such as antistatic coatings and for half of the samples, conductivity reaches the requirements for electronic conductive inks. The results for the graphene compacts and paper film suggest that the maximum conductivity reachable at such low effective densities lies around 10^4 S m^{-1}. Taking into account the varied synthesis methods and dimensional characteristics, the conductivity results shown in Figure 25 are fairly consistent with a conductivity model based on the percolation theory.

Composites elaborated through *in situ* polymerization exhibit lower effective densities than in the physical blends due to lower filler contents. Some physical blending procedures provide access to high conductivities.[96,162]

7. Conclusions and Outlook

Heterophase polymerization techniques are widely used for the synthesis of high performance polymeric materials with applications including paints, coatings, inks, adhesives, synthetic rubber, biomedical applications and many others. There are also industrially relevant tools for the production of graphene-based nanocomposites. As emphasized in this review, one of the main advantages of heterophase polymerization is the possibility to tailor both surface and volume properties. This allows the elaboration of polymer/graphene nanocomposites in a simple manner by the physical blending of preformed latex particles and graphenic fillers. The segregated network morphology of the final composite blend is secured by electrostatic or π stacking interactions between the graphenic fillers and the latex particles. The majority of studies in this area have not involved "pristine" graphene, but rather carbon materials produced by the reduction of GO because of the proven scalability and ease of these methods. However, recent studies have shown that graphite can be exfoliated in liquid media into few-layer or even monolayer graphene and with further development, such methods may be scalable. Consequently, FLG, GO and RGO can be indifferently used for latex blending. The second reviewed method is *in situ* polymerization. All three main heterophase polymerization processes (*i.e.*, emulsion, suspension and miniemulsion polymerizations) have been reported with more or less success using almost exclusively GO nanosheets as graphenic filler (with the exception of two papers). Indeed, as alluded to above, GO is hydrophilic and is known to disperse well in water. Its hydrophilicity is mainly attributed to the ionizable edges. Furthermore, its basal plane is composed of hydrophobic un-oxidized benzene rings, which confers it an amphiphilic character. This amphiphilicity drives the GO platelets to solid/liquid or liquid/liquid interfaces allowing *in situ* stabilization of latex particles or miniemulsion and suspension droplets with subsequent formation of armored particles and a variety of hybrid morphologies depending on the sheet lateral dimensions and the size of the latex particles. Other heterogeneous polymerization approaches like microemulsion or precipitation polymerizations have also been investigated but these studies are still marginal. The Pickering miniemulsion polymerization approach also proved efficient for the synthesis of hybrid

capsules consisting of a cross-linked polymer shell and a GO coating opening the door to exotic structures, which are novel building blocks for the elaboration of complex multifunctional materials.

When elaborating composite materials from building blocks, the morphology of the building block itself is a parameter to consider. In particular the size ratio between the latex diameter and the graphene sheet lateral size influences the final morphology. For graphenic fillers smaller or slightly larger than the latex particles, a cellular morphology is expected. If the lateral size of the graphenic filler is strongly larger than the latex diameter, a segregated network is also obtained but self-alignment might occur at high filler content, due to steric hindrance of the wide graphene sheets. Several parameters were shown to influence the mechanical and electrical properties of graphene-based latex nanocomposites. In particular, storage modulus was shown to increase as the filler concentration increased and the percolation threshold decreased as the latex particle size increased. However no work so far reports the effect of the size distribution of graphene sheets on properties while Thickett *et al.*[10] reported that the synthesis of GO is not yet highly reproducible in terms of size distribution. Moreover the use of GO induces the need for a reduction step that has been shown not to fully recover the conductive properties. Moreover, the presence of the latex particles can give rise to a slight additional decrease in the reduction efficiency. Thus, in order to favor higher conductivity in the final composite, the use of pristine graphene sheets in the composite elaboration or the development of more efficient reduction processes are potential future improvements still to be explored.

Work on graphene/polymer latex nanocomposites is in its early stages and there is still considerable work that needs to be done to optimize their synthesis, microstructure and physical properties. Nevertheless, property enhancements of graphene-latex nanocomposites have been well demonstrated and the maturity of latex industry for low cost and large-scale production should favor their transfer to the marketplace in applications such as electronics devices, energy storage, sensors, electromagnetic shielding and biomedical applications.

8. Acknowledgments

Drs. Samuel Pearson and Ming Liang Koh (C2P2) are gratefully acknowledged for their help during the preparation of this manuscript.

9. List of Abbreviations

AA	acrylic acid
AFM	atomic force microscopy
AIBN	2,2'-azobis(isobutyronitrile)
AMPS	2-acrylamido-2-methyl-1-propanesulfonic acid
APS	ammonium persulfate
BA	*n*-butyl acrylate
CB	carbon black
CMC	critical micelle concentration
CNTs	carbon nanotubes
CTAB	cetyl trimethylammonium bromide
CVD	chemical vapor deposition
DIBTC	dodecyl isobutyric acid trithiocarbonate
DLS	dynamic light scattering
DSC	differential scanning calorimetry
Đ	dispersity (previously polydispersity index)
D_h	hydrodynamic diameter
DMF	dimethyl formamide
DVB	divinylbenzene
EG	expanded graphene
EI	ethyleneimine
FLG	few-layer graphene
GNS	graphene nanosheets
GO	graphene oxide
HD	hexadecane
HEA	hydroxyethyl acrylate
HEC	hydroxyethylcellulose
HEMA	hydroxyethyl methacrylate
HI	hydrogen iodine
HREM	high-resolution electron microscopy

FNG	functionalized graphene
FTIR	Fourier-transform infrared
GNP	graphene nanoplatelets
KPS	potassium persulfate
LbL	layer-by-layer
MLG	multilayer graphene
MMA	methyl methacrylate
NMG	nanosized multilayer graphene
NMP	N-methylpyrrolidone
PMDETA	N,N,N',N",N"-pentamethyldiethylenetriamine
NR	natural rubber
OP-10	poly(ethylene oxide)octylphenyl ether surfactant with 10 oxyethylene
PAN	polyacrylonitrile
PANI	polyaniline
PC	polycarbonate
PDADMAC	poly(diallyldimethylammonium chloride)
PDMAEMA	poly(dimethylaminoethyl methacrylate)
PEI	polyethyleneimine
PMMA	poly(methyl methacrylate)
PP	polypropylene
PPy	polypyrrole
PSD	particle size distribution
PSSNa	sodium poly(styrene sulfonate)
PTFE	polytetrafluoroethylene
PVA	poly(vinyl alcohol)
PVAc	poly(vinyl acetate)
PVP	poly(N-vinyl pyrrolidone)
RAFT	reversible addition fragmentation chain transfer polymerization
RGO	reduced graphene oxide
St	styrene

SBR	styrene-butadiene rubber
SDBS	sodium dodecyl benzene sulfonate
SDS	sodium dodecyl sulfate
SEM	scanning electron microscopy
SSNa	sodium styrene sulfonate
TEM	transmission electron microscopy
TGA	thermal gravimetric analysis
T_g	glass transition temperature
THF	tetrahydrofuran
VAc	vinyl acetate
VdW	Van der Waals
WAXD	wide angle x-ray diffraction
XPS	X-ray photoelectron spectroscopy

10. References

1. Novoselov, K. S.; Geim, A. K.; Morozov, S. V.; Jiang, D.; Zhang, Y.; Dubonos, S. V.; Grigorieva, I. V.; Firsov, A. A., Electric Field Effect in Atomically Thin Carbon Films. *Science* **2004,** *306*, 666-669.
2. (a) Allen, M. J.; Tung, V. C.; Kaner, R. B., Honeycomb carbon: a review of graphene. *Chem. Rev.* **2010,** *110* (1), 132-45; (b) Park, S.; Ruoff, R. S., Chemical methods for the production of graphenes. *Nat. Nanotechnol.* **2009,** *4* (4), 217-224; (c) Soldano, C.; Mahmood, A.; Dujardin, E., Production, properties and potential of graphene. *Carbon* **2010,** *48* (8), 2127-2150.
3. Cai, M.; Thorpe, D.; Adamson, D. H.; Schniepp, H. C., Methods of graphite exfoliation. *J. Mater. Chem.* **2012,** *22* (48), 24992-25002.
4. (a) Dreyer, D. R.; Park, S.; Bielawski, C. W.; Ruoff, R. S., The chemistry of graphene oxide. *Chem. Soc. Rev.* **2010,** *39* (1), 228-240; (b) Eigler, S.; Hirsch, A., Chemistry with Graphene and Graphene Oxide— Challenges for Synthetic Chemists. *Angew. Chem. Int. Ed.* **2014,** *53*, 7720-7738; (c) Kuila, T.; Bose, S.; Mishra, A. K.; Khanra, P.; Kim, N. H.; Lee, J. H., Chemical functionalization of graphene and its applications. *Prog. Mater. Sci.* **2012,** *57* (7), 1061-1105; (d) Quintana, M.; Vazquez, E.; Prato, M., Organic Functionalization of Graphene in Dispersions. *Acc. Chem. Res.* **2013,** *46* (1), 138-148.
5. (a) Geim, A. K., Graphene: Status and Prospects. *Science* **2009,** *324*, 1530-1534; (b) Zhu, Y.; Murali, S.; Cai, W.; Li, X.; Suk, J. W.; Potts, J. R.; Ruoff, R. S., Graphene and graphene oxide: synthesis, properties, and applications. *Adv. Mater.* **2010,** *22* (35), 3906-3924.

6. (a) Bai, H.; Li, C.; Shi, G., Functional composite materials based on chemically converted graphene. *Adv. Mater.* **2011,** *23* (9), 1089-1115; (b) Du, J.; Cheng, H.-M., The Fabrication, Properties, and Uses of Graphene/Polymer Composites. *Macromol. Chem. Phys.* **2012,** *213* (10-11), 1060-1077; (c) Mittal, G.; Dhand, V.; Rhee, K. Y.; Park, S.-J.; Lee, W. R., A review on carbon nanotubes and graphene as fillers in reinforced polymer nanocomposites. *J. Ind. Eng. Chem.* **2015,** *21*, 11-25; (d) Hu, K.; Kulkarni, D. D.; Choi, I.; Tsukruk, V. V., Graphene-polymer nanocomposites for structural and functional applications. *Prog. Polym. Sci.* **2014,** *39*, 1934-1972; (e) Kuilla, T.; Bhadra, S.; Yao, D.; Kim, N. H.; Bose, S.; Lee, J. H., Recent advances in graphene based polymer composites. *Prog. Polym. Sci.* **2010,** *35* (11), 1350-1375; (f) Notley, S. M.; Evans, D. R., Aqueous processing of graphene–polymer hybrid thin film nano-composites and gels. *Adv. Colloid Interf. Sci.* **2014,** *209*, 196-203; (g) Potts, J. R.; Dreyer, D. R.; Bielawski, C. W.; Ruoff, R. S., Graphene-based polymer nanocomposites. *Polymer* **2011,** *52* (1), 5-25.
7. Kim, H.; Abdala, A. A.; Macosko, C. W., Graphene/Polymer Nanocomposites. *Macromolecules* **2010,** *43* (16), 6515-6530.
8. Suspension polymerization leads to the formation of polymer beads with sizes typically of the order of 10 μm to 5 mm in diameter which is outside the latex particle size range (i.e. 50-500 nm). Therefore, in suspension polymerization, the resulting product is not strictly speaking a latex suspension. However, the size of the suspension droplets can be decreased by high shear mixing or sonication resulting in the formation of fine particles which are in the colloidal size range of latex particles.
9. Bourgeat-Lami, E.; Lansalot, M., Organic/Inorganic Composite Latexes: The Marriage of Emulsion Polymerization and Inorganic Chemistry. *Adv. Polym. Sci.* **2010,** *233*, 53-123.
10. Thickett, S.; Zetterlund, P., Functionalization of Graphene Oxide for the Production of Novel Graphene-Based Polymeric and Colloidal Materials. *Curr. Org. Chem.* **2013,** *17*, 956-974.
11. Das, T. K.; Prusty, S., Graphene-Based Polymer Composites and Their Applications. *Polym-Plast. Technol.* **2013,** *52* (4), 319-331.
12. Kumar, A.; Lee, C. H., *Synthesis and Biomedical Applications of Graphene: Present and Future Trends, Advances in Graphene Science*. InTech: 2013.
13. Castro Neto, A. H.; Peres, N. M. R.; Novoselov, K. S.; Geim, A. K., The electronic properties of graphene. *Rev. Mod. Phys.* **2009,** *81* (1), 109-162.
14. Craciun, M. F.; Russo, S.; Yamamoto, M.; Tarucha, S., Tuneable electronic properties in graphene. *Nano Today* **2011,** *6* (1), 42-60.
15. Hummers, W. S.; Offeman, R. E., Preparation of graphitic oxide. *J. Am. Chem. Soc.* **1958,** *80*, 1339.
16. Li, X.; Zhang, G.; Bai, X.; Sun, X.; Wang, X.; Wang, E.; Dai, H., Highly conducting graphene sheets and Langmuir-Blodgett films. *Nat. Nanotechnol.* **2008,** *3* (9), 538-542.
17. Li, D.; Muller, M. B.; Gilje, S.; Kaner, R. B.; Wallace, G. G., Processable aqueous dispersions of graphene nanosheets. *Nat. Nanotechnol.* **2007,** *3* (2), 101-105.
18. Si, Y.; Samulski, E. T., Synthesis of Water Soluble Graphene. *Nano letters* **2008,** *8* (6), 1679-1682.
19. Schniepp, H. C.; Li, J.-L.; McAllister, M. J.; Sai, H.; Herrera-Alonso, M.; Adamson, D. H.; Prud'homme, R. K.; Car, R.; Saville, D. A.; Aksay, I. A., Functionalized Single Graphene Sheets Derived from Splitting Graphite Oxide. *J. Phys. Chem. B* **2006,** *110*, 8535-8539.
20. Khan, U.; Porwal, H.; O'Neill, A.; Nawaz, K.; May, P.; Coleman, J. N., Solvent-exfoliated graphene at extremely high concentration. *Langmuir* **2011,** *27* (15), 9077-9082.

21. McAllister, M. J.; Li, J.-L.; Adamson, D. H.; Schniepp, H. C.; Abdala, A. A.; Liu, J.; Herrera-Alonso, M.; Milius, D. L.; Car, R.; Prud'homme, R. K.; Aksay, I. A., Single Sheet Functionalized Graphene by Oxidation and Thermal Expansion of Graphite. *Chem. Mater.* **2007,** *19*, 4396-4404.
22. Zhang, L.; Liang, J.; Huang, Y.; Ma, Y.; Wang, Y.; Chen, Y., Size-controlled synthesis of graphene oxide sheets on a large scale using chemical exfoliation. *Carbon* **2009,** *47* (14), 3365-3368.
23. Latif, I.; B. Alwan, T.; H. Al-Dujaili, A., Low Frequency Dielectric Study of PAPA-PVA-GR Nanocomposites. *Nanoscience and Nanotechnology* **2013,** *2* (6), 190-200.
24. Chen, W.; Yan, L.; Bangal, P. R., Chemical Reduction of Graphene Oxide to Graphene by Sulfur-Containing Compounds. *J. Phys. Chem. C* **2010,** *114*, 19885-19890.
25. Zhou, X.; Zhang, J.; Wu, H.; Yang, H.; Zhang, J.; Guo, S., Reducing Graphene Oxide via Hydroxylamine: A Simple and Efficient Route to Graphene. *J. Phys. Chem. C* **2011,** *115* (24), 11957-11961.
26. Fernandez-Merino, M. J.; Guardia, L.; Paredes, J. I.; Villar-Rodil, S.; Solıs-Fernandez, P.; Martınez-Alonso, A.; Tascon, J. M. D., Vitamin C Is an Ideal Substitute for Hydrazine in the Reduction of Graphene Oxide Suspensions. *J. Phys. Chem. C* **2010,** *114*, 6426-6432.
27. Dubin, S.; Gilje, S.; Wang, K.; Tung, V. C.; Cha, K.; Hall, A. S.; Farrar, J.; Varshneya, R.; Yang, Y.; Kaner, R. B., A One-Step, Solvothermal Reduction Method for Producing Reduced Graphene Oxide Dispersions in Organic Solvents. *ACS Nano* **2010,** *4* (7), 3845-3582.
28. Zhang, Y.; Ma, H.-L.; Zhang, Q.; Peng, J.; Li, J.; Zhai, M.; Yu, Z.-Z., Facile synthesis of well-dispersed graphene by γ-ray induced reduction of graphene oxide. *J. Mater. Chem.* **2012,** *22* (26), 13064-13069.
29. Stankovich, S.; Dikin, D. A.; Piner, R. D.; Kohlhaas, K. A.; Kleinhammes, A.; Jia, Y.; Wu, Y.; Nguyen, S. T.; Ruoff, R. S., Synthesis of graphene-based nanosheets via chemical reduction of exfoliated graphite oxide. *Carbon* **2007,** *45* (7), 1558-1565.
30. Buglione, L.; Chng, E. L. K.; Ambrosi, A.; Sofer, Z.; Pumera, M., Graphene materials preparation methods have dramatic influence upon their capacitance. *Electrochem. Commun.* **2012,** *14* (1), 5-8.
31. Cheng, M.; Yang, R.; Zhang, L.; Shi, Z.; Yang, W.; Wang, D.; Xie, G.; Shi, D.; Zhang, G., Restoration of graphene from graphene oxide by defect repair. *Carbon* **2012,** *50* (7), 2581-2587.
32. Zhang, H.-B.; Zheng, W.-G.; Yan, Q.; Jiang, Z.-G.; Yu, Z.-Z., The effect of surface chemistry of graphene on rheological and electrical properties of polymethylmethacrylate composites. *Carbon* **2012,** *50* (14), 5117-5125.
33. Hernandez, Y.; Nicolosi, V.; Lotya, M.; Blighe, F. M.; Sun, Z.; De, S.; McGovern, I. T.; Holland, B.; Byrne, M.; Gun'Ko, Y. K.; Boland, J. J.; Niraj, P.; Duesberg, G.; Krishnamurthy, S.; Goodhue, R.; Hutchison, J.; Scardaci, V.; Ferrari, A. C.; Coleman, J. N., High-yield production of graphene by liquid-phase exfoliation of graphite. *Nat. Nanotechnol.* **2008,** *3* (9), 563-568.
34. Nixon, D. E.; Parry, G. S., Formation and structure of the potassium graphites. *Brit. J. Appl. Phys.* **1968,** *1*, 291-298.
35. Catheline, A.; Valles, C.; Drummond, C.; Ortolani, L.; Morandi, V.; Marcaccio, M.; Iurlo, M.; Paolucci, F.; Penicaud, A., Graphene solutions. *Chem. Commun.* **2011,** *47* (19), 5470-5472.
36. Zhao, W.; Wu, F.; Wu, H.; Chen, G., Preparation of Colloidal Dispersions of Graphene Sheets in Organic Solvents by Using Ball Milling. *J. Nanomater.* **2010**, e528235.
37. An, X.; Simmons, T.; Shah, R.; Wolfe, C.; Lewis, K. M.; Washington, M.; Nayak, S. K.; Talapatra, S.; Kar, S., Stable aqueous dispersions of noncovalently functionalized

graphene from graphite and their multifunctional high-performance applications. *Nano letters* **2010,** *10* (11), 4295-4301.
38. Guardia, L.; Fernández-Merino, M. J.; Paredes, J. I.; Solís-Fernández, P.; Villar-Rodil, S.; Martínez-Alonso, A.; Tascón, J. M. D., High-throughput production of pristine graphene in an aqueous dispersion assisted by non-ionic surfactants. *Carbon* **2011,** *49* (5), 1653-1662.
39. Lotya, M.; Hernandez, Y.; King, P. J.; Smith, R. J.; Nicolosi, V.; Karlsson, L. S.; Blighe, F. M.; De, S.; Wang, Z.; McGovern, I. T.; Duesberg, G. S.; Coleman, J. N., Liquid Phase Production of Graphene by Exfoliation of Graphite in Surfactant/Water Solutions. *J. Am. Chem. Soc.* **2009,** *131*, 3611-3620.
40. Lee, J. H.; Shin, D. W.; Makotchenko, V. G.; Nazarov, A. S.; Fedorov, V. E.; Yoo, J. H.; Yu, S. M.; Choi, J. Y.; Kim, J. M.; Yoo, J. B., The superior dispersion of easily soluble graphite. *Small* **2010,** *6* (1), 58-62.
41. Knieke, C.; Berger, A.; Voigt, M.; Taylor, R. N. K.; Röhrl, J.; Peukert, W., Scalable production of graphene sheets by mechanical delamination. *Carbon* **2010,** *48* (11), 3196-3204.
42. Novoselov, K. S.; Geim, A. K.; Morozov, S. V.; Jiang, D.; Katsnelson, M. I.; Grigorieva, I. V.; Dubonos, S. V.; Firsov, A. A., Two-dimensional gas of massless Dirac fermions in graphene. *Nature* **2005,** *438* (7065), 197-200.
43. Nair, R. R.; Blake, P.; Grigorenko, A.; Novoselov, K. S.; Booth, T. J.; Stauber, T.; Peres, N. M. R.; Geim, A. K., Fine Structure Constant Defines Visual Transparency of Graphene. *Science* **2008,** *320*, 1308.
44. Bolotin, K. I.; Sikes, K. J.; Jiang, Z.; Klima, M.; Fudenberg, G.; Hone, J.; Kim, P.; Stormer, H. L., Ultrahigh electron mobility in suspended graphene. *Solid State Commun.* **2008,** *146* (9-10), 351-355.
45. Baladin, A. A.; Ghosh, S.; Bao, W.; Calizo, I.; Teweldebrhan, D.; Miao, F.; Lau, C. N., Superior Thermal Conductivity of Single-Layer Graphene. *Nano letters* **2008,** *8*, 902-907.
46. Hu, K.; Kulkarni, D. D.; Choi, I.; Tsukruk, V. V., Graphene-polymer nanocomposites for structural and functional applications. *Prog. Polym. Sci.* **2014,** *39* (11), 1934-1972.
47. Mousavi, H.; Khodadadi, J., Flake electrical conductivity of few-layer graphene. *Sci. World J.* **2014,** *2014*, e581478.
48. Lee, C.; Wei, X.; Kysar, J. W.; Hone, J., Measurement of the Elastic Properties and Intrinsic Strength of Monolayer Graphene. *Science* **2008,** *321*, 385-388.
49. Frank, I. W.; Tanenbaum, D. M.; van der Zande, A. M.; McEuen, P. L., Mechanical properties of suspended graphene sheets. *Journal of Vacuum Science &Technology B* **2007,** *25* (6), 2558-2561.
50. Wang, Z.; Xie, R.; Bui, C. T.; Liu, D.; Ni, X.; Li, B.; Thong, J. T., Thermal transport in suspended and supported few-layer graphene. *Nano letters* **2011,** *11* (1), 113-118.
51. Chen, W.; Yan, L.; Bangal, P. R., Preparation of graphene by the rapid and mild thermal reduction of graphene oxide induced by microwaves. *Carbon* **2010,** *48* (4), 1146-1152.
52. Falkovsky, L. A., Optical properties of graphene. *J. Phys. Conf. Ser.* **2008,** *129*, 012004.
53. Park, H. J.; Meyer, J.; Roth, S.; Skákalová, V., Growth and properties of few-layer graphene prepared by chemical vapor deposition. *Carbon* **2010,** *48* (4), 1088-1094.
54. Banhart, F.; Kotakoski, J.; Krasheninnikov, A. V., Structural Defects in Graphene. *ACS Nano* **2011,** *5* (1), 26-41.
55. Yan, L.; Zheng, Y. B.; Zhao, F.; Li, S.; Gao, X.; Xu, B.; Weiss, P. S.; Zhao, Y., Chemistry and physics of a single atomic layer: strategies and challenges for functionalization of graphene and graphene-based materials. *Chem. Soc. Rev.* **2012,** *41* (1), 97-114.

56. Boukhvalov, D. W.; Katsnelson, M. I., Chemical Functionalization of Graphene with Defects. *Nanolett.* **2008,** *8*, 4373-4379.
57. Peng, X.; Ahuja, R., Symmetry Breaking Induced Bandgap in Epitaxial Graphene Layers on SiC. *Nano letters* **2008,** *8* (12), 4464-4468.
58. Loh, K. P.; Bao, Q.; Ang, P. K.; Yang, J., The chemistry of graphene. *J. Mater. Chem.* **2010,** *20*, 2277-2289.
59. Levy, M.; Szwarc, M., Reactivities of Aromatic Hydrocarbons toward Methyl Radicals. *J. Am. Chem. Soc.* **1955,** *77*, 1949-1955.
60. Hey, D. H.; Williams, G. H., Partial rate factors for homolytic aromatic substitution *Discuss. Faraday Soc.* **1953,** *14*, 216-221.
61. Hayashi, S.; Handa, S.; Oshibe, Y.; Yamamoto, T.; Tsubokawa, N., Grafting of polymers onto carbon black surface by the trapping of polymer radicals formed by the decomposition of peroxide polymers. *Polym. J.* **1995,** *27* (6), 623-630.
62. Wakai, H.; Shinno, T.; Yamauchi, T.; Tsubokawa, N., Grafting of poly(ethylene oxide) onto C60 fullerene using macroazo initiators. *Polymer* **2007,** *48* (7), 1972-1980.
63. Beckert, F.; Rostas, A. M.; Thomann, R.; Weber, S.; Schleicher, E.; Friedrich, C.; Mülhaupt, R., Self-Initiated Free Radical Grafting of Styrene Homo- and Copolymers onto Functionalized Graphene. *Macromolecules* **2013,** *46* (14), 5488-5496.
64. Ohkita, K.; Tsubokawa, N.; Saitoh, E., The Competitive reactions of initiator fragments and growing polymer chains against the surface of carbon black *Carbon* **1978,** *16*, 41-45.
65. Shen, B.; Zhai, W.; Chen, C.; Lu, D.; Wang, J.; Zheng, W., Melt blending in situ enhances the interaction between polystyrene and graphene through pi-pi stacking. *ACS Appl. Mater. Inter.* **2011,** *3* (8), 3103-3109.
66. Stankovich, S.; Dikin, D. A.; Dommett, G. H.; Kohlhaas, K. M.; Zimney, E. J.; Stach, E. A.; Piner, R. D.; Nguyen, S. T.; Ruoff, R. S., Graphene-based composite materials. *Nature* **2006,** *442* (7100), 282-286.
67. Liu, J.; Tao, L.; Yang, W.; Li, D.; Boyer, C.; Wuhrer, R.; Braet, F.; Davis, T. P., Synthesis, characterization, and multilayer assembly of pH sensitive graphene-polymer nanocomposites. *Langmuir* **2010,** *26* (12), 10068-10075.
68. Salavagione, H. J.; Gómez, M. n. A.; Martínez, G., Polymeric Modification of Graphene through Esterification of Graphite Oxide and Poly(vinyl alcohol). *Macromolecules* **2009,** *42* (17), 6331-6334.
69. Liu, Z.; Robinson, J. T.; Sun, X.; Dai, H., PEGylated Nanographene Oxide for Delivery of Water-Insoluble Cancer Drugs. *J. Am. Chem. Soc.* **2008,** *130*, 10876-10877.
70. Wang, J.-Y.; Yang, S.-Y.; Huang, Y.-L.; Tien, H.-W.; Chin, W.-K.; Ma, C.-C. M., Preparation and properties of graphene oxide/polyimide composite films with low dielectric constant and ultrahigh strength via in situ polymerization. *J. Mater. Chem.* **2011,** *21* (35), 13569-13575.
71. Pham, T. A.; Kumar, N. A.; Jeong, Y. T., Covalent functionalization of graphene oxide with polyglycerol and their use as templates for anchoring magnetic nanoparticles. *Synth. Met.* **2010,** *160* (17-18), 2028-2036.
72. Ren, P.-G.; Yan, D.-X.; Chen, T.; Zeng, B.-Q.; Li, Z.-M., Improved properties of highly oriented graphene/polymer nanocomposites. *J. Appl. Polym. Sci.* **2011,** *121* (6), 3167-3174.
73. Goncalves, G.; Marques, P. A. A. P.; Barros-Timmons, A.; Bdkin, I.; Singh, M. K.; Emami, N.; Gracio, J., Graphene oxide modified with PMMA via ATRP as a reinforcement filler. *J. Mater. Chem.* **2010,** *20* (44), 9927-9934.

74. (a) Vivaldo-Lima, E.; Wood, P. E.; Hamielec, A. E., An Updated Review on Suspension Polymerization. *Ind. Eng. Chem. Res.* **1997,** *36*, 939-965; (b) Brooks, B., Suspension Polymerization Processes. *Chem. Eng. Technol.* **2010,** *33* (11), 1737-1744.
75. (a) Asua, J. M., Emulsion Polymerization: From Fundamental Mechanisms to Process Developments. *J. Polym. Sci. Polym. Chem.* **2004,** *42*, 1025-1041; (b) Chern, C. S., Emulsion polymerization mechanisms and kinetics. *Prog. Polym. Sci.* **2006,** *31* (5), 443-486.
76. Colver, P. J.; Colard, C. A. L.; Bon, S. A. F., Multilayered Nanocomposite Polymer Colloids Using Emulsion Polymerization Stabilized by Solid Particles. *J. Am. Chem. Soc.* **2008,** *130*, 16850-16851.
77. Sheibat-Othman, N.; Bourgeat-Lami, E., Use of silica particles for the formation of organic-inorganic particles by surfactant-free emulsion polymerization. *Langmuir* **2009,** *25* (17), 10121-10133.
78. Bourgeat-Lami, E.; Guimaraes, T. R.; Pereira, A. M.; Alves, G. M.; Moreira, J. C.; Putaux, J. L.; Dos Santos, A. M., High solids content, soap-free, film-forming latexes stabilized by laponite clay platelets. *Macromol. Rapid Commun.* **2010,** *31* (21), 1874-1880.
79. Teixeira, R. F. A.; McKenzie, H. S.; Boyd, A. A.; Bon, S. A. F., Pickering Emulsion Polymerization Using Laponite Clay as Stabilizer To Prepare Armored "Soft" Polymer Latexes. *Macromolecules* **2011,** *44* (18), 7415-7422.
80. Kim, Y. J.; Liu, Y. D.; Seo, Y.; Choi, H. J., Pickering-Emulsion-Polymerized Polystyrene/Fe2O3 Composite Particles and Their Magnetoresponsive Characteristics. *Langmuir* **2013,** *29*, 4959-4965.
81. Asua, J. M., Miniemulsion polymerization. *Prog. Polym. Sci.* **2002,** *27* (7), 1283-1346.
82. Bon, S. A. F.; Colver, P. J., Pickering Miniemulsion Polymerization Using Laponite Clay as a Stabilizer. *Langmuir* **2007,** *23*, 8316-8322.
83. Zgheib, N.; Putaux, J. L.; Thill, A.; D'Agosto, F.; Lansalot, M.; Bourgeat-Lami, E., Stabilization of miniemulsion droplets by cerium oxide nanoparticles: a step toward the elaboration of armored composite latexes. *Langmuir* **2012,** *28* (14), 6163-6174.
84. Pickering, S. U., Emulsions. *J. Chem. Soc. Trans.* **1907,** *91*, 2001-2021.
85. (a) Barrett, K. E. J., *Dispersion Polymerization in Organic Media*. John Wiley & Sons, Inc.,: New York, 1975; (b) Barrett, K. E. J., Dispersion polymerization in organic media. *Br. Polym. J.* **1973,** *5*, 259-271.
86. Fan, W.; Zhang, C.; Tjiu, W. W.; Liu, T., Fabrication of electrically conductive graphene/polystyrene composites via a combination of latex and layer-by-layer assembly approaches. *J. Mater. Res.* **2013,** *28* (4), 611-619.
87. Long, G.; Tang, C.; Wong, K.-w.; Man, C.; Fan, M.; Lau, W.-m.; Xu, T.; Wang, B., Resolving the dilemma of gaining conductivity but losing environmental friendliness in producing polystyrene/graphene composites via optimizing the matrix-filler structure. *Green Chem.* **2013,** *15* (3), 821-828.
88. Noel, A.; Faucheu, J.; Rieu, M.; Viricelle, J.-P.; Bourgeat-Lami, E., Tunable architecture for flexible and highly conductive graphene-polymer composites. *Compos. Sci. Technol.* **2014,** *95*, 82-88.
89. Yoonessi, M.; Gaier, J. R., Highly Conductive Multifunctional Graphene Polycarbonate Nanocomposites. *ACS Nano* **2010,** *4*, 7211-7220.
90. Tang, C.; Long, G.; Hu, X.; Wong, K.-w.; Lau, W.-m.; Fan, M.; Mei, J.; Xu, T.; Wang, B.; Hui, D., Conductive polymer nanocomposites with hierarchical multi-scale structures via self-assembly of carbon-nanotubes on graphene on polymer-microspheres. *Nanoscale* **2014,** *6* (14), 7877-7888.
91. Wakabayashi, K.; Pierre, C.; Dikin, D. A.; Ruoff, R. S.; Ramanathan, T.; Brinson, L. C.; Torkelson, J. M., Polymer-Graphite Nanocomposites: Effective Dispersion and Major

Property Enhancement via Solid-State Shear Pulverization. *Macromolecules* **2008,** *41*, 1905-1908.
92. Matos, C. F.; Galembeck, F.; Zarbin, A. J. G., Multifunctional and environmentally friendly nanocomposites between natural rubber and graphene or graphene oxide. *Carbon* **2014,** *78*, 469-479.
93. Arzac, A.; Leal, G. P.; Fajgar, R.; Tomovska, R., Comparison of the Emulsion Mixing and In Situ Polymerization Techniques for Synthesis of Water-Borne Reduced Graphene Oxide/Polymer Composites: Advantages and Drawbacks. *Part. Part. Syst. Char.* **2014,** *31* (1), 143-151.
94. Zhan, Y.; Lavorgna, M.; Buonocore, G.; Xia, H., Enhancing electrical conductivity of rubber composites by constructing interconnected network of self-assembled graphene with latex mixing. *J. Mater. Chem.* **2012,** *22* (21), 10464-10468.
95. Zhao, P.; Luo, Y.; Yang, J.; He, D.; Kong, L.; Zheng, P.; Yang, Q., Electrically conductive graphene-filled polymer composites with well organized three-dimensional microstructure. *Mater. Lett.* **2014,** *121*, 74-77.
96. Wu, C.; Huang, X.; Wang, G.; Lu, L.; Chen, G.; Li, G.; Jiang, P., Highly Conductive Nanocomposites with Three- Dimensional, Compactly Interconnected Graphene Networks via a Self-Assembly Process. *Adv. Funct. Mater.* **2013,** *23*, 506-513.
97. Li, H.; Wu, S.; Wu, J.; Huang, G., A facile approach to the fabrication of graphene-based nanocomposites by latex mixing and in situ reduction. *Colloid Polym. Sci.* **2013,** *291* (10), 2279-2287.
98. Jiang, H.; Chen, L.; Chai, S.; Yao, X.; Chen, F.; Fu, Q., Facile fabrication of poly (tetrafluoroethylene)/graphene nanocomposite via electrostatic self-assembly approach. *Compos. Sci. Technol.* **2014,** *103*, 28-35.
99. Pham, V. H.; Dang, T. T.; Hur, S. H.; Kim, E. J.; Chung, J. S., Highly Conductive Poly(methyl methacrylate) (PMMA)-Reduced Graphene Oxide Composite Prepared by Self-Assembly of PMMA Latex and Graphene Oxide through Electrostatic Interaction. *ACS Appl. Mater. Inter.* **2012,** *4* (5), 2630-2636.
100. Yousefi, N.; Gudarzi, M. M.; Zheng, Q.; Aboutalebi, S. H.; Sharif, F.; Kim, J.-K., Self-alignment and high electrical conductivity of ultralarge graphene oxide–polyurethane nanocomposites. *J. Mater. Chem.* **2012,** *22*, 12709-12717.
101. Wang, D.; Zhang, X.; Zha, J.-W.; Zhao, J.; Dang, Z.-M.; Hu, G.-H., Dielectric properties of reduced graphene oxide/polypropylene composites with ultralow percolation threshold. *Polymer* **2013,** *54*, 1916-1922.
102. Zhang, W. L.; Liu, Y. D.; Choi, H. J.; Seo, Y., Core-shell structured graphene oxide-adsorbed anisotropic poly(methyl methacrylate) microparticles and their electrorheology. *RSC Adv.* **2013,** *3* (29), 11723-11731.
103. Kim, J.; Cote, L. J.; Kim, F.; Yuan, W.; Shull, K. R.; Huang, J., Graphene Oxide Sheets at Interfaces. *J. Am. Chem. Soc.* **2010,** *132*, 8180-8186.
104. Gudarzi, M. M.; Sharif, F., Molecular level dispersion of graphene in polymer matrices using colloidal polymer and graphene. *J. Colloid Interf. Sci.* **2012,** *366* (1), 44-50.
105. Zhang, T.; Li, X.; Kang, S.; Qin, L.; Yan, W.; Mu, J., Facile assembly and properties of polystyrene microsphere/reduced graphene oxide/Ag composite. *J. Colloid Interf. Sci.* **2013,** *402*, 279-283.
106. Yang, Y.; Wang, J.; Zhang, J.; Liu, J.; Yang, X.; Zhao, H., Exfoliated Graphite Oxide Decorated by PDMAEMA Chains and Polymer Particles. *Langmuir* **2009,** *25* (19), 11808-11814.
107. Mechrez, G.; Suckeveriene, R. Y.; Segal, E.; Narkis, M., Polymer/carbon nanofillers films fabricated by latex technology. *Polym. Adv. Technol.* **2014,** *25*, 1301-1306.

108. Ghislandi, M.; Tkalya, E.; Marinho, B.; Koning, C. E.; de With, G., Electrical conductivities of carbon powder nanofillers and their latex-based polymer composites. *Compos. Part A. Appl. S.* **2013,** *53*, 145-151.
109. Pinto, A. M.; Martins, J.; Moreira, J. A.; Mendes, A. M.; Magalhaes, F. D., Dispersion of graphene nanoplatelets in poly(vinyl acetate) latex and effect on adhesive bond strength. *Polym. Int.* **2012,** *62*, 928-935.
110. Ju, S. A.; Kim, K.; Kim, J. H.; Lee, S. S., Graphene-wrapped hybrid spheres of electrical conductivity. *ACS Appl. Mater. Interfaces* **2011,** *3* (8), 2904-2911.
111. Syurik, Y. V.; Ghislandi, M. G.; Tkalya, E. E.; Paterson, G.; McGrouther, D.; Ageev, O. A.; Loos, J., Graphene Network Organisation in Conductive Polymer Composites. *Macromol. Chem. Phys.* **2012,** *213*, 1251-1258.
112. Spasevska, D.; Daniloska, V.; Leal, G. P.; Gilev, J. B.; Tomovska, R., Reactive emulsion mixing as a novel pathway toward water-borne reduced graphene oxide/polymer composites. *RSC Adv.* **2014,** *4* (47), 24477-24483.
113. Jiang, S.; Gui, Z.; Bao, C.; Dai, K.; Wang, X.; Zhou, K.; Shi, Y.; Lo, S.; Hu, Y., Preparation of functionalized graphene by simultaneous reduction and surface modification and its polymethyl methacrylate composites through latex technology and melt blending. *Chem. Eng. J.* **2013,** *226* (0), 326-335.
114. Tchernook, A.; Krumova, M.; Tölle, F. J.; Mülhaupt, R.; Mecking, S., Composites from Aqueous Polyethylene Nanocrystal/Graphene Dispersions. *Macromolecules* **2014,** *47* (9), 3017-3021.
115. Rippel, M. M.; Lee, L.-T.; Leite, C. A. P.; Galembeck, F., Skim and cream natural rubber particles: colloidal properties, coalescence and film formation. *J. Colloid Interf. Sci.* **2003,** *268* (2), 330-340.
116. Li, C.; Feng, C.; Peng, Z.; Gong, W.; Kong, L., Ammonium-assisted green fabrication of graphene/natural rubber latex composite. *Polym. Composite* **2013,** *34* (1), 88-95.
117. Zhan, Y. L., M.; Buonocore, G.; Xia, H., Enhancing electrical conductivity of rubber composites by constructing interconnected network of self-assembled graphene with latex mixing. *J. Mater. Chem.* **2012,** *22*, 10464-10468.
118. Yan, N.; Buonocore, G.; Lavorgna, M.; Kaciulis, S.; Balijepalli, S. K.; Zhan, Y.; Xia, H.; Ambrosio, L., The role of reduced graphene oxide on chemical, mechanical and barrier properties of natural rubber composites. *Compos. Sci. Technol.* **2014,** *102*, 74-81.
119. Zhan, Y.; Wu, J.; Xia, H.; Yan, N.; Fei, G.; Yuan, G., Dispersion and Exfoliation of Graphene in Rubber by an Ultrasonically-Assisted Latex Mixing and In situ Reduction Process. *Macromol. Mater. Eng.* **2011,** *296* (7), 590-602.
120. Potts, J. R.; Shankar, O.; Murali, S.; Du, L.; Ruoff, R. S., Latex and two-roll mill processing of thermally-exfoliated graphite oxide/natural rubber nanocomposites. *Compos. Sci. Technol.* **2013,** *74*, 166-172.
121. Luo, Y.; Zhao, P.; Yang, Q.; He, D.; Kong, L.; Peng, Z., Fabrication of conductive elastic nanocomposites via framing intact interconnected graphene networks. *Compos. Sci. Technol.* **2014,** *100*, 143-151.
122. Xing, W. T., M.; Wu, J.; Huang, G.; Li, H.; Lei, Z.; Fu, X.; Li, H., Multifunctional properties of graphene/rubber nanocomposites fabricated by a modified latex compounding method. *Compos. Sci. Technol.* **2014,** *99*, 67-74.
123. Mao, Y.; Zhang, S.; Zhang, D.; Chan, T. W.; Liu, L., Enhancing graphene oxide reinforcing potential in composites by combined latex compounding and spray drying. *Materials Research Express* **2014,** *1* (2), 025009.
124. Tian, M.; Zhang, J.; Zhang, L.; Liu, S.; Zan, X.; Nishi, T.; Ning, N., Graphene encapsulated rubber latex composites with high dielectric constant, low dielectric loss and low percolation threshold. *J. Colloid Interf. Sci.* **2014,** *430*, 249-56.

125. Yousefi, N.; Lin, X.; Zheng, Q.; Shen, X.; Pothnis, J. R.; Jia, J.; Zussman, E.; Kim, J.-K., Simultaneous in situ reduction, self-alignment and covalent bonding in graphene oxide/epoxy composites. *Carbon* **2013,** *59*, 406-417.
126. (a) Kim, J.; Cote, L. J.; Huang, J., Two Dimensional Soft Material: New Faces of Graphene Oxide. *Acc. Chem. Res.* **2012,** *45* (8), 1356-1365; (b) Zhang, W. L.; Choi, H. J., Graphene oxide based smart fluids. *Soft Matter.* **2014,** *10* (35), 6601-6608.
127. (a) He, Y.; Wu, F.; Sun, X.; Li, R.; Guo, Y.; Li, C.; Zhang, L.; Xing, F.; Wang, W.; Gao, J., Factors that Affect Pickering Emulsions Stabilized by Graphene Oxide. *ACS Appl. Mater. Interfaces* **2013,** *5*, 4843-4855; (b) Thickett, S. C.; Zetterlund, P. B., Graphene oxide (GO) nanosheets as oil-in-water emulsion stabilizers: Influence of oil phase polarity. *J. Colloid Interf. Sci.* **2015,** *442* (0), 67-74.
128. Ding, R.; Hu, Y.; Gui, Z.; Zong, R.; Chen, Z.; Fan, W., Preparation and characterization of polystyrene/graphite oxide nanocomposite by emulsion polymerization. *Polym. Degrad. Stabil.* **2003,** *81* (3), 473-476.
129. Zhang, R.; Hu, Y.; Xu, J.; Fan, W.; Chen, Z., Flammability and thermal stability studies of styrene–butyl acrylate copolymer/graphite oxide nanocomposite. *Polym. Degrad. Stabil.* **2004,** *85* (1), 583-588.
130. Wang, W.-P.; Pan, C.-Y., Preparation and characterization of poly(methyl methacrylate)-intercalated graphite oxide/poly(methyl methacrylate) nanocomposite. *Polym. Eng. Sci.* **2004,** *44* (12), 2335-2339.
131. Hu, H.; Wang, X.; Wang, J.; Wan, L.; Liu, F.; Zheng, H.; Chen, R.; Xu, C., Preparation and properties of graphene nanosheets–polystyrene nanocomposites via in situ emulsion polymerization. *Chem. Phys. Lett.* **2010,** *484* (4–6), 247-253.
132. Glover, A. J.; Adamson, D. H.; Schniepp, H. C., Charge-Driven Selective Adsorption of Sodium Dodecyl Sulfate on Graphene Oxide Visualized by Atomic Force Microscopy. *J. Phys. Chem. C* **2012,** *116* (37), 20080-20085.
133. Yang, J.; Shi, G.; Tu, Y.; Fang, H., High correlation between oxidation loci on graphene oxide. *Angew. Chem. Int. Ed.* **2014,** *53* (38), 10190-10194.
134. Hsieh, A. G.; Korkut, S.; Punckt, C.; Aksay, I. A., Dispersion stability of functionalized graphene in aqueous sodium dodecyl sulfate solutions. *Langmuir* **2013,** *29* (48), 14831-14838.
135. Hsieh, A. G.; Punckt, C.; Korkut, S.; Aksay, I. A., Adsorption of sodium dodecyl sulfate on functionalized graphene measured by conductometric titration. *J. Phys. Chem. B* **2013,** *117* (26), 7950-7958.
136. Kattimuttathu, S. I.; Krishnappan, C.; Vellorathekkaepadil, V.; Nutenki, R.; Mandapati, V. R.; Černík, M., Synthesis, characterization and optical properties of graphene oxide-polystyrene nanocomposites. *Polym. Adv. Technol.* **2015,** *26*, 214-222.
137. Thickett, S. C.; Zetterlund, P. B., Preparation of Composite Materials by Using Graphene Oxide as a Surfactant in Ab Initio Emulsion Polymerization Systems. *ACS Macro Lett.* **2013,** *2* (7), 630-634.
138. Yin, G.; Zheng, Z.; Wang, H.; Du, Q.; Zhang, H., Preparation of graphene oxide coated polystyrene microspheres by Pickering emulsion polymerization. *Journal of Colloid and Interface Science* **2013,** *394*, 192-198.
139. Yeole, N.; Kutcherlapati, S. N.; Jana, T., Polystyrene-graphene oxide (GO) nanocomposite synthesized by interfacial interactions between RAFT modified GO and core-shell polymeric nanoparticles. *J. Colloid Interf. Sci.* **2015,** *443*, 137-42.
140. Xie, P.; Ge, X.; Fang, B.; Li, Z.; Liang, Y.; Yang, C., Pickering emulsion polymerization of graphene oxide-stabilized styrene. *Colloid Polym. Sci.* **2013,** *291*, 1631-1639.

141. Hassan, M.; Reddy, K. R.; Haque, E.; Minett, A. I.; Gomes, V. G., High-yield aqueous phase exfoliation of graphene for facile nanocomposite synthesis via emulsion polymerization. *J. Colloid Interf. Sci.* **2013,** *410*, 43-51.
142. Lee, J.; Hong, J.; Shim, S. E., Miniemulsion Polymerization of Styrene in the Presence of Graphite Nanosheets. *Macromol. Res.* **2009,** *17* (11), 931-933.
143. Etmimi, H. M.; Mallon, P. E., In situ exfoliation of graphite oxide nanosheets in polymer nanocomposites using miniemulsion polymerization. *Polymer* **2013,** *54* (22), 6078-6088.
144. Etmimi, H. M.; Mallon, P. E.; Sanderson, R. D., Polymer/graphite nanocomposites: Effect of reducing the functional groups of graphite oxide on water barrier properties. *Eur. Polym. J.* **2013,** *49* (11), 3460-3470.
145. Che Man, S.; Thickett, S.; Whittaker, M.; Zetterlund, P., Synthesis of polystyrene nanoparticles "armoured" with nanodimensional graphene oxide sheets by miniemulsion polymerization. *J. Polym. Sci. Polym. Chem.* **2013,** *51* (1), 47-58.
146. Kim, F.; Cote, L. J.; Huang, J., Graphene oxide: surface activity and two-dimensional assembly. *Adv. Mater.* **2010,** *22* (17), 1954-1958.
147. Luo, J.; Cote, L. J.; Tung, V. C.; Tan, A. T. L.; Goins, P. E.; Wu, J.; Huang, J., Graphene Oxide Nanocolloids. *J. Am. Chem. Soc.* **2010,** *132*, 17667-17669.
148. Che Man, S. H.; Mohd Yusof, N. Y.; Whittaker, M. R.; Thickett, S. C.; Zetterlund, P. B., Influence of monomer type on miniemulsion polymerization systems stabilized by graphene oxide as sole surfactant. *J. Polym. Sci. Polym. Chem.* **2013,** *51* (23), 5153-5162.
149. Che Man, S. H.; Ly, D.; Whittaker, M. R.; Thickett, S. C.; Zetterlund, P. B., Nano-sized graphene oxide as sole surfactant in miniemulsion polymerization for nanocomposite synthesis: Effect of pH and ionic strength. *Polymer* **2014,** *55* (16), 3490-3497.
150. Thickett, S. C.; Wood, N.; Ng, Y. H.; Zetterlund, P. B., Hollow hybrid polymer-graphene oxide nanoparticles via Pickering miniemulsion polymerization. *Nanoscale* **2014,** *6* (15), 8590-8594.
151. Etmimi, H. M.; Tonge, M. P.; Sanderson, R. D., Synthesis and characterization of polystyrene-graphite nanocomposites via surface RAFT-mediated miniemulsion polymerization. *J. Polym. Sci. Polym. Chem.* **2011,** *49* (7), 1621-1632.
152. Etmimi Hussein M, S. R. D., New Approach to the Synthesis of Exfoliated Polymer/Graphite Nanocomposites by Miniemulsion Polymerization Using Functionalized Graphene. *Macromolecules* **2011,** *44*, 8504-8515.
153. Gudarzi, M. M.; Sharif, F., Self assembly of graphene oxide at the liquid–liquid interface: A new route to the fabrication of graphene based composites. *Soft Matter* **2011,** *7* (7), 3432-3440.
154. Song, X.; Yang, Y.; Liu, J.; Zhao, H., PS colloidal particles stabilized by graphene oxide. *Langmuir* **2011,** *27* (3), 1186-1191.
155. Xuemei, H.; Hao, Y., Fabrication of Polystyrene/Detonation Nanographite Composite Microspheres with the Core/Shell Structure via Pickering Emulsion Polymerization. *J. Nanomater.* **2013**, 751497.
156. Kim, S. D.; Zhang, W. L.; Choi, H. J., Pickering emulsion-fabricated polystyrene–graphene oxide microspheres and their electrorheology. *J. Mater. Chem. C* **2014,** *2* (36), 7541-7546.
157. Dao, T. D.; Erdenedelger, G.; Jeong, H. M., Water-dispersible graphene designed as a Pickering stabilizer for the suspension polymerization of poly(methyl methacrylate)/graphene core–shell microsphere exhibiting ultra-low percolation threshold of electrical conductivity. *Polymer* **2014,** *55* (18), 4709-4719.

158. Patole, A. S.; Patole, S. P.; Kang, H.; Yoo, J.-B.; Kim, T.-H.; Ahn, J.-H., A facile approach to the fabrication of graphene/polystyrene nanocomposite by in situ microemulsion polymerization. *J. Colloid Interf. Sci.* **2010,** *350* (2), 530-537.
159. Patole, A. S.; Patole, S. P.; Jung, S.-Y.; Yoo, J.-B.; An, J.-H.; Kim, T.-H., Self assembled graphene/carbon nanotube/polystyrene hybrid nanocomposite by in situ microemulsion polymerization. *Eur. Polym. J.* **2012,** *48* (2), 252-259.
160. Thomassin, J.-M.; Trifkovic, M.; Alkarmo, W.; Detrembleur, C.; Jérôme, C.; Macosko, C., Poly(methyl methacrylate)/Graphene Oxide Nanocomposites by a Precipitation Polymerization Process and Their Dielectric and Rheological Characterization. *Macromolecules* **2014,** *47* (6), 2149-2155.
161. Stauffer, D.; Aharony, A., *Introduction to Percolation Theory*. London, Washington, DC, 1992; p 974.
162. Noël, A.; Faucheu, J.; Chenal, J.-M.; Viricelle, J.-P.; Bourgeat-Lami, E., Electrical and mechanical percolation in graphene-latex nanocomposites. *Polymer* **2014,** *55* (20), 5140-5145.
163. Pötschke, P.; Abdel-Goad, M.; Pegel, S.; Jehnichen, D.; Mark, J. E.; Zhou, D.; Heinrich, G., Comparisons Among Electrical and Rheological Properties of Melt-Mixed Composites Containing Various Carbon Nanostructures. *J. Macromol. Sci. A* **2009,** *47* (1), 12-19.
164. Rittigstein, P.; Priestley, R. D.; Broadbelt, L. J.; Torkelson, J. M., Model polymer nanocomposites provide an understanding of confinement effects in real nanocomposites. *Nat. Mater.* **2007,** *6* (4), 278-82.
165. Du, F.; Scogna, R. C.; Zhou, W.; Brand, S.; Fischer, J. E.; Winey, K. I., Nanotube Networks in Polymer Nanocomposites: Rheology and Electrical Conductivity. *Macromolecules* **2004,** *37*, 9048-9055.
166. Hicks, J.; Behnam, A.; Ural, A., A computational study of tunneling-percolation electrical transport in graphene-based nanocomposites. *Appl. Phys. Lett.* **2009,** *95* (21), 213103.
167. Li, J.; Kim, J.-K., Percolation threshold of conducting polymer composites containing 3D randomly distributed graphite nanoplatelets. *Compos. Sci. Technol.* **2007,** *67* (10), 2114-2120.
168. Moriarty, G. P.; Whittemore, J. H.; Sun, K. A.; Rawlins, J. W.; Grunlan, J. C., Influence of Polymer Particle Size on the Percolation Threshold of Electrically Conductive Latex-Based Composites. *J. Polym. Sci. Polym. Phys.* **2011,** *49*, 1547-1554.
169. Francis, L. F.; Grunlan, J. C.; Sun, J.; Gerberich, W. W., Conductive coatings and composites from latex-based dispersions. *Colloid Surface A* **2007,** *311* (1-3), 48-54.
170. Kim, Y. S.; Wright, J. B.; Grunlan, J. C., Influence of polymer modulus on the percolation threshold of latex-based composites. *Polymer* **2008,** *49* (2), 570-578.
171. Yi, Y.; Tawerghi, E., Geometric percolation thresholds of interpenetrating plates in three-dimensional space. *Phys. Rev. E* **2009,** *79* (4), E 79, 041134.
172. Chen, J.-H.; Jang, C.; Xiao, S.; Ishigami, M.; Fuhrer, M. S., Intrinsic and extrinsic performance limits of graphene devices on SiO2. *Nat. Nanotechnol.* **2008,** *3* (4), 206-209.